# Identifying pyroclastic density currents from partial outcrop exposure on Mt Ruapehu, New Zealand

Masters in Geology

Department of Geological Sciences, University of Canterbury

New Zealand

**Janina Gillies**

2018

## Acknowledgements

This Masters thesis would not have been possible without the amazing support I received throughout my research. I am grateful to my supervisors Ben Kennedy, Darren Gravley, and Graham Leonard, who provided guidance and invaluable knowledge during this project and kept me motivated with their enthusiasm and belief in me. Ben Kennedy, who directed me through my first few days of field work, and has provided valuable time and feedback. Graham Leonard, as well as Dougal Townsend, gave me an introduction to working on Mt Ruapehu and supplied me with the resources and knowledge to begin my research. Thanks too to Thomas Wilson who helped to direct this project and for keeping me on track. I am also exceptionally grateful to James Cowlyn, whose previous work on Mt Ruapehu paved the path for this thesis, and whose advice and expertise on Ruapehu proved indispensable to shaping this project.

Laboratory processing of samples was made easier by the help of the UC technical staff, especially Rob Spiers who made all of my many thin sections, and Chris Grimshaw who allowed me to take over the sedimentology laboratory and built equipment needed during this study. Also thanks to Sacha Baldwin who helped prepare me for the field. I am also extremely grateful for the help of Anja Moebis and Georg Zellmer from Massey University who showed me how to prepare my geochemistry samples and were very patient and understanding during my many technical issues.

Field work on Mt Ruapehu by myself would have been tough, so I am very thankful for the field assistance provided by Janina Adolf, Tom Brough, and Steph Gates, who made field work even more fun and passed on valuable skills and knowledge.

My time on Ruapehu was also made more enjoyable by Don French and the Tukino Alpine Sports Club who made their ski lodge available to me during much of my field work and provided a comfortable place to recuperate after long field days. Also, thanks to Justyna Giejsztowt, the resident biologist and my taxi driver, who kept me sane with homecooked food, and company.

A special thanks to the Department of Conservation, Ngāti Rangi and other local iwi who allowed access and sampling. Especially Hollei Gabrielsen for her support and assistance while I was on Ruapehu by making sure that I was safe, and respecting cultural traditions.

I would also like to acknowledge the very generous support of the Project Tongariro Memorial Award and the University of Canterbury Mason Trust Fund. This project would not have been possible without these sources of funding.

Finally, a huge thank you to everyone in the University of Canterbury Geological Sciences Depatment for their continued support, and to my friends and family for their encouragement when things were tough and for their unwavering belief in me.

## Abstract

Mt Ruapehu is one of New Zealand's most active volcanoes, last erupting in 2007. There have been few studies investigating the pyroclastic density current (PDC) hazard for Mt Ruapehu, despite being a popular tourist attraction. Due to the unpredictability of this hazard, it is crucial to be aware of past events in order to produce an effective plan for future PDCs.

On Mt Ruapehu, poor preservation of pyroclastic material due to past glaciations, erosion, and poor consolidation has led to significant uncertainty in distinguishing PDC deposits. This thesis aims to provide a rapid methodology to classify PDCs when doing whole volcano–scale mapping with limited sampling options. Multiple techniques in the field and laboratory were used to identify and characterise these deposits, and to create broad–scale implications for PDC frequency and magnitude. Comprehensive field-mapping over three months formed the basis for this study by identifying potential PDCs from partial exposures. A confidence-based pyroclastic identification chart developed by Cowlyn (2016) was used to support interpretations based on diagnostic textures of PDCs. Grain size distribution, vesicularity, and geochemical analyses of samples have been used to correlate deposits and infer the eruption style. The magnitude and volume of flows have been approximated using a digital elevation model and estimated flow paths.

This study identified 14 PDCs, adding to the 12 previously characterised by Cowlyn (2016). 50% of the PDCs identified occurred during Plinian to sub-plinian eruptions based on the deposit sizes and textural properties. These formed large volume, pumice-dominated deposits. 36% of the PDCS were likely formed during Strombolian eruptions when accumulated spatter underwent gravitational collapse. This eruption style formed variably welded, thermally altered, spatter-rich deposits with denser clasts. The remaining 14% of PDCs formed during smaller, Vulcanian eruptions, creating small volume, scoria-dominated deposits. The results from this study have been integrated into a map with the identified

PDC deposits and an updated account of PDC occurrence for Mt Ruapehu. Increasing the awareness of past PDCs can help inform hazard management and provide a foundation for subsequent studies to investigate future PDC scenarios on Mt Ruapehu.

# Contents

## 1. Introduction

With an increasing population, urbanisation, and infrastructure over the last 50 years, natural hazards such as volcanic eruptions are posing a greater threat to society (Johnston et al. 2000). Therefore, it is crucial to fully understand these hazards in order to reduce the impact they have on society. This is especially important in areas with large numbers of people, such as Mt Ruapehu, New Zealand, where up to 10,000 people can be present on the mountain during peak times (Nairn et al. 1996). Pyroclastic density currents (PDC) are one example of a volcanic hazard that threatens populations proximal to the volcano, contributing to 33% of fatalities during natural disasters since 1600 AD (Auker et al. 2013).

While the occurrence of PDCs on Mt Ruapehu has been briefly mentioned in past literature, little investigation has been conducted into their occurrence and frequency (Hackett 1985; Donoghue et al. 1995; Pardo 2012; Townsend et al. 2017). Prior to the study conducted by Cowlyn (2016), who identifed multiple PDCs on the eastern side of Mt Ruapehu, the PDC hazard was often overlooked (Figure 1), primarily due to a lack of historic PDCs and the poor preservation of prehistoric PDCs. Small to medium sized unconsolidated PDCs have a low preservation potential, especially when deposited on steep slopes and in active drainages for water and ice (Manville et al. 2000; Cowlyn 2016). This makes it difficult to locate and identify PDC deposits, leading to an unknown PDC hazard on Mt Ruapehu, increasing the overall risk that they pose to the area.

The overall goal of this study is to enhance the knowledge of the frequency and magnitude of PDCs on Mt Ruapehu by identifying and correlating more deposits. Mt Ruapehu was chosen due to the large tourism industry and visitor numbers each year and the lack of knowledge of the PDC occurrence over the entire volcano. A variety of field and laboratory techniques are used to conduct this study. These include textural and relative stratigraphic observations of outcrops, a confidence-based PDC identification chart created by Cowlyn

(2016), grain size distribution, density and vesicularity analyses, and whole rock major element geochemistry.

The aims directing this project were:

- Identify PDC deposits through comprehensive field mapping and diagnostic textural characteristics. A confidence-based pyroclastic identification chart developed by Cowlyn (2016) supported this identification.
- Group the PDCs by type and age using relative stratigraphic locations, textural characteristics and bulk geochemistry.
- Infer the eruption style that formed the PDCs using textural characteristics and international analogues
- Extrapolate deposits based on palaeotopography assumptions to estimate volumes and potential run out distances.

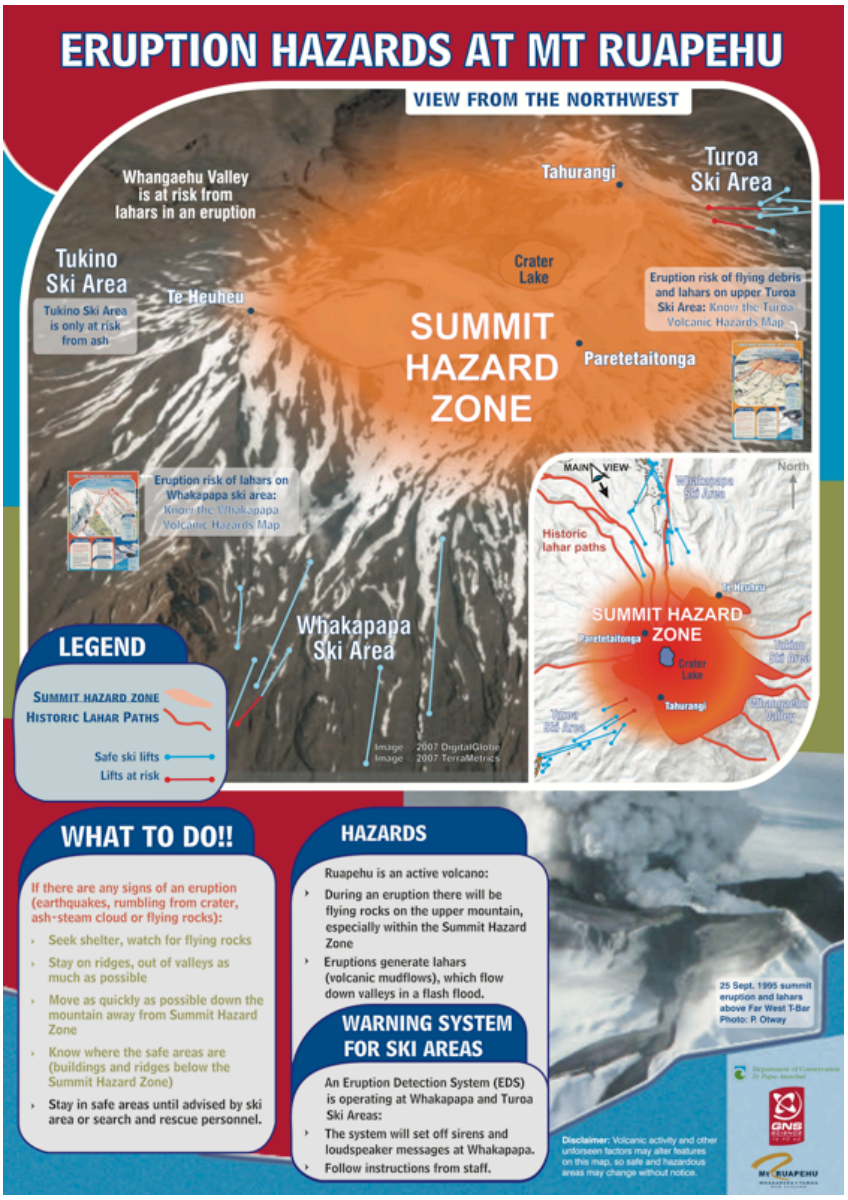


**Figure 1. The current hazard map for Mt Ruapehu (GNS Science). There is no mention of a PDC hazard occurring on Mt Ruapehu.**

## 1.1 Pyroclastic density currents

Pyroclastic density currents (PDCs) are volcanic hazards that occur during explosive eruptions and can result in considerable damage to anything that they interact with as they travel away from the vent. PDCs are rapidly moving turbulent mixtures of hot gas, and juvenile and non-juvenile volcanic particles, that flow under the influence of gravity and can reach velocities of over 100km/h

(Buchwaldt 2013). The deposits of these flows are usually emplaced at temperatures between 200-600°C (Brown & Andrews 2015).

Several different mechanisms are capable of producing these flows: gravitational collapse of a lava dome, an explosion within a lava dome triggering an eruption, the collapse of the toe of flowing lava, collapse of accumulated Strombolian spatter, and the collapse of an eruption column, such as Plinian or Vulcanian (Valentine et al. 2000; Stinton & Sheridan 2008; Buchwaldt 2013).

Pumiceous PDCs formed during a Plinian/sub-plinian column collapse are often of evolved compositions (Brown & Andrews 2015). They are known to contain an abundance of ash and pumice, with pumice clasts abrasively rounded during transport (Brown & Andrews 2015). These flows are categorised as "pumiceous" if they contain highly vesicular material (Buchwaldt 2013). Pumice clasts in these flows often have densities between 0.2-1 g/cm$^3$ (Brown & Andrews 2015), though this range may vary.

Small volume PDCs (< $10^7$ m$^3$) from column collapse during Vulcanian eruptions can cover a large compositional range, from basaltic to rhyolitic (Stinton & Sheridan 2008; Brown & Andrews 2015). These are called scoriaceous when the juvenile clasts are moderately vesicular (Buchwaldt 2013). An example of this type of flow is the 1975 Ngauruhoe eruption which produced multiple PDCs. Deposits from this eruption were andesitic, with densities between 1.1-1.3 g/cm$^3$, and 'cauliflower' shaped clasts with 'breadcrusted' textures (Nairn & Self 1978). Scoria clasts from other examples have displayed densities between 1-2 g/cm$^3$ (Brown & Andrews 2015).

Spatter-fed PDCs, formed during Strombolian eruptions where the erupted spatter travels downslope, are usually composed of dense to vesicular scoria or spatter lapilli and bombs. The spatter clasts may be imbricated, and show evidence of emplacement while hot and ductile (Brown & Andrews 2015). These deposits are usually found in areas close to the vent (Brown & Andrews 2015).

A PDC can be divided into two distinct end-members: a diluted suspension of particles carried by gas, “pyroclastic surge”, and a thicker, fluidized, granular “pyroclastic flow” where there is a greater concentration of particles (Fisher & Schmincke 1984; Roche et al. 2013). Most PDCs consist of a granular flow with an overriding surge, complicating their behaviour (Roche et al. 2013). The gravitational collapse of lava domes form a block and ash flow, a subset of smaller PDCs with a higher particle concentration (Brown & Andrews 2015). This study will focus on the larger pyroclastic flows that have the greatest chance of preservation in the geological record and travel the furthest.

Pyroclastic surges can travel up to approximately 8 km from the source vent and are usually not confined to valleys as it travels downslope, buoyancy allowing the surges to overtop topography and impact the surrounding environment (Buchwaldt 2013). Pyroclastic flows, however, are often confined to valleys and can travel up to 100 km away from the vent during large eruptions (Buchwaldt 2013). An example of the devastation that PDCs can cause is the 2010 Mt Merapi pyroclastic flow where 380 people were killed and over 2200 buildings were damaged (Cronin et al. 2013; Jenkins et al. 2013). Block and ash flows travelled over 16 km from the source and spread out downstream where there were fewer valleys, causing greater damage.

The high velocity, high temperature, and great distances mean that this volcanic hazard poses a significant risk to nearby communities and infrastructure. Over the 20$^{th}$ Century, PDCs accounted for the largest proportion of deaths from volcanic eruptions (Witham 2005). In particular, PDCs on Mt Ruapehu would be hazardous due to the high concentration of visitors on the mountain and the proximity of the people to the source of the hazard—chairlifts carry skiers to within 2 km of the vent (Nairn et al. 1996).

## 1.2 Geological setting

Mt Ruapehu is located at the southern end of the Taupo Volcanic Zone (TVZ) (Figure 2), a rifted arc formed from the oblique subduction of the Pacific Plate underneath the Australian Plate (Cole 1990; Wilson et al. 1995).

Volcanic activity in the TVZ began approximately 2 Ma with andesitic eruptions forming composite cones in the northern and southern segments (Wilson et al. 1995; Conway et al. 2016). Volumetrically dominant rhyolitic eruptions later began at 1.6 Ma, forming the central part of the TVZ. At the southern end of the TVZ is the Tongariro Volcanic Centre (TgVC), where the volcanic arc is best developed (Cole 1990). This volcanic centre consists of four large, generally andesitic, volcanoes: Kakaramea, Pihanga, Tongariro, and Ruapehu, in addition to other smaller cones.

Mt Ruapehu (2797m) is an active, andesite-dacite, composite volcano with a volume of approximately 150 $km^3$ (Hackett & Houghton 1989). This volcano began erupting at approximately 250 ka and consists of four formations: Te Herenga (250-180 ka), Wahianoa (160-115 ka), Mangawhero (55-20 ka), and Whakapapa (15-2 ka) (Hackett & Houghton 1989; Price et al. 2012). While the oldest lava flows are dated at approximately 200 ka, there is evidence in debris flow deposits of an older mountain, that now may be buried or eroded, erupting at least 340 ka (Tost & Cronin 2015).

Ruapehu is characterised by a series of intense constructional events separated by periods of erosion, sector collapse, and minor volcanic activity (Price et al. 2012). There is an apparent hiatus in eruptive activity from 80-50 ka (Townsend et al. 2017). Compositions range from basalt to dacite with predominantly medium *K* andesite (Hackett & Houghton 1989). More evolved compositions and a wider compositional range has been erupted over time (Hackett & Houghton 1989). The single, currently active vent is located in the southern portion of the broad summit, and forms the acidic Crater Lake/Te Wai-ā-moe (Hackett & Houghton 1989).

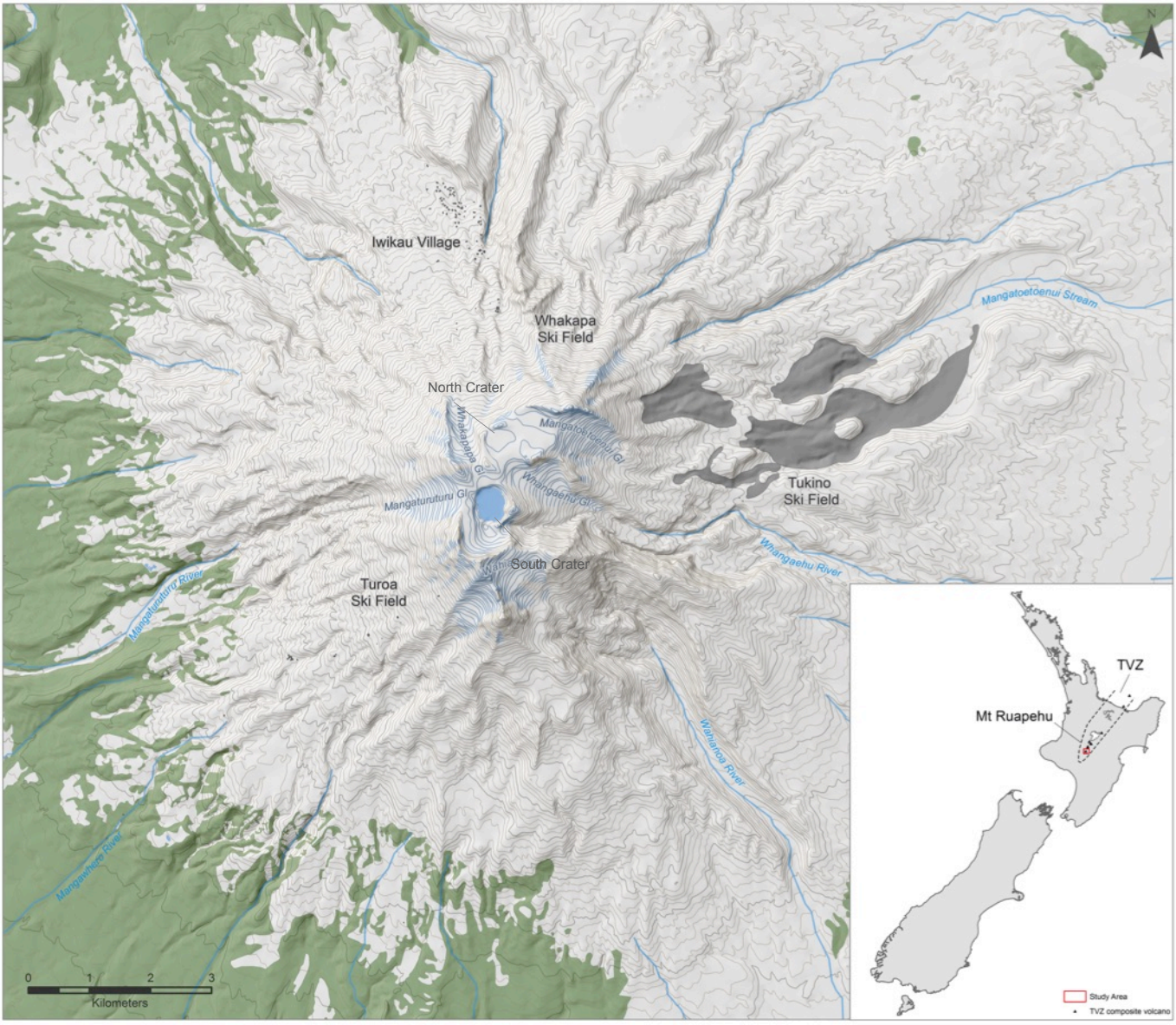


**Figure 2. Topographic map of Mt Ruapehu with skifields and PDCs identified by Cowlyn (2016) (dark grey). Previous vent (North Crater), and current vent (South Crater) are marked. Inset shows location of Mt Ruapehu within New Zealand and the TVZ. Map data gathered from https://data.linz.govt.nz.**

## 1.3 Eruptive history

Mt Ruapehu has been erupting in short, intense periods for the last 250 ka, which is characteristic behaviour for arc type volcanoes (Gamble et al. 1999; Price et al. 2012). Variability in composition between events indicates that mixing and mingling has occurred within the volcanic edifice between the fresh magma and stagnant magma remaining from previous activity (Gamble et al. 1999). This shows that Mt Ruapehu is supplied by an open magma system. The geochemical

composition of eruptive products is variable, and does not evolve consistently over time (Figure 3). Townsend et al. (2017) describes a gradual increase in $SiO_2$ between 200-80 ka. In later formations, the compositional range is greater, though generally higher in $SiO_2$. From approximately 35 ka onwards there was a trend towards more mafic eruptions, though the Crater Lake Formation (<4.6 ka) displays the complete $SiO_2$ range seen throughout the eruptive history (Conway et al. 2016; Townsend et al. 2017). The eruptive vent locations have also varied over time, with a shift at ~11.6 ka from large Plinian-style eruptions occurring from the North Crater (Figure 2), to smaller scale activity from a vent close to, or at, the current South Crater (Pardo et al. 2012b; Pardo et al. 2012a; Cowlyn 2016).

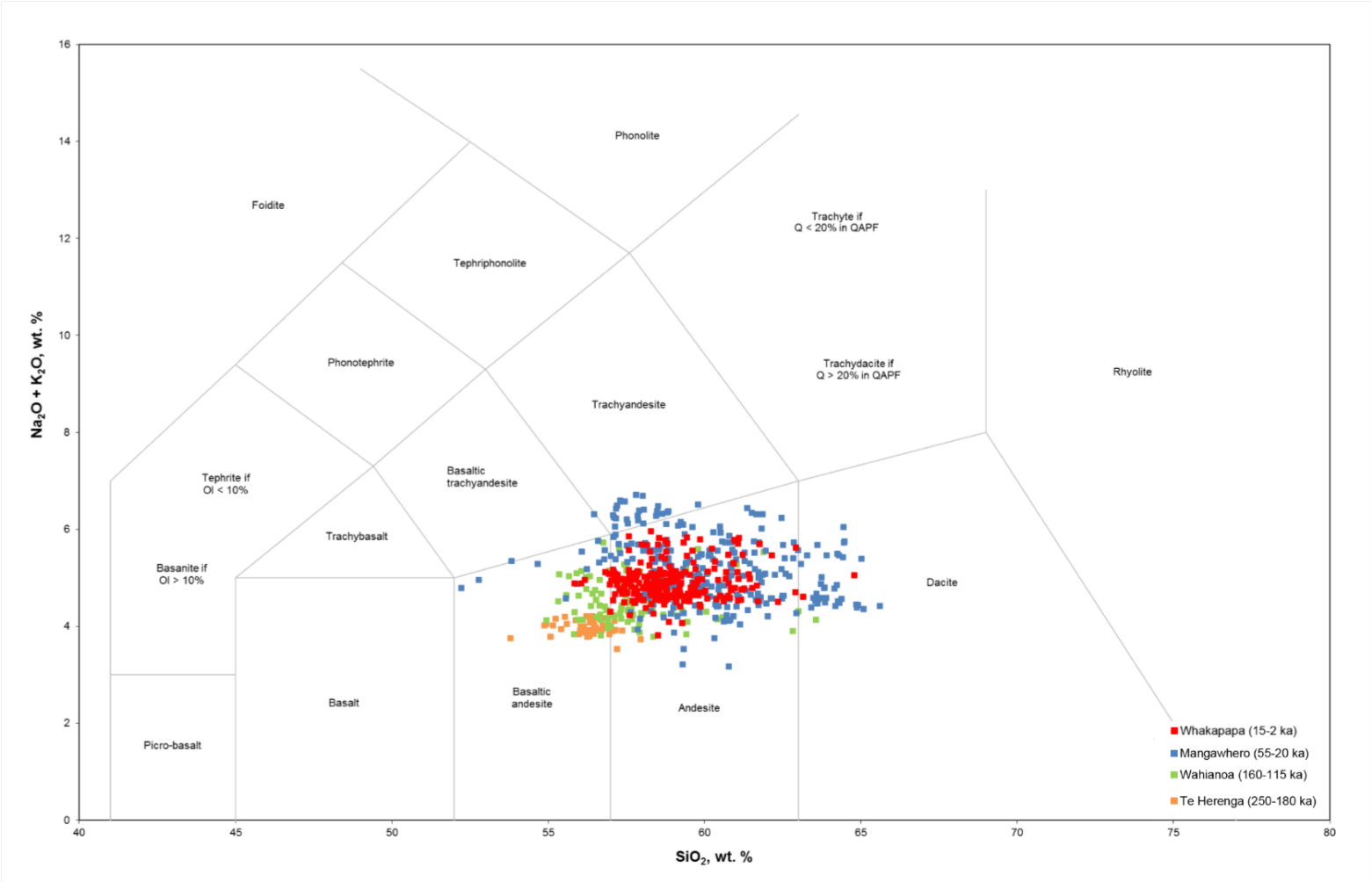


**Figure 3. Geochemistry of Mt Ruape formations. There is an overall gradual increase in $SiO_2$ between the Te Herenga Formation (250-180 ka) and the Mangawhero Formation (55-20 ka). After 15 ka the $SiO_2$ content decreases (Whakapapa Formation). Data gathered from Price et al. (2012).**

Throughout its formation, eruptive activity at Mt Ruapehu has been characterised by Plinian, sub-plinian, Strombolian, phreatomagmatic, Vulcanian, dome-related explosivity, and the extrusion of lava flows and domes (Hackett & Houghton 1989; Pardo 2012). Over the last 150 years the most frequently observed eruption types include phreatomagmatic and phreatic activity, with a larger lava-dome explosion event in 1945 that occurred during an eruptive period also associated with sub-plinian and Strombolian eruption styles (Johnston et al. 2000). More than 40 eruptions have occurred since then (Kilgour et al. 2013). Based on these eruptions an average, long-term recurrence interval of 4.00 or 0.49 events per year has been calculated, depending whether all eruptions since 1940 are taken into account, or if the larger 1945 and 1995-1996 activity is excluded, respectively (Scott 2013).

Sequences forming the cone of the volcano are predominantly lava flows, both blocky and A'a (Hackett & Houghton 1989). The deposits forming the ring plain, however, primarily consist of explosive pyroclastics, such as ashfall, and reworked material from the cone, such as lahar (Hackett & Houghton 1989).

The unpredictability of a wide range of volcanism at Mt Ruapehu means that it is difficult to judge when another eruption may occur and what style; therefore, it is nearly impossible to fully prepare for the subsequent volcanic hazards.

### 1.4 Pyroclastic density currents on Mt Ruapehu

A photograph of Mt Ruapehu during the 1945 eruption provides evidence of the occurrence of PDCs by showing a small flow travelling down the southern slopes (Figure 4), though there was no recording of the event. Despite evidence of the occurrence of PDCs on Mt Ruapehu little research has been done on the PDCs at Mt Ruapehu due to the poor preservation and absence of reported historic occurrences causing an unknown hazard frequency. Donoghue et al. (1995) is one of the few studies that mentioned PDCs on Mt Ruapehu. In that study,

evidence of a magma mingling episode was identified in the juvenile material of a PDC within the Bullot Formation. Donoghue et al. (1995) determined that due to poor preservation of unconsolidated PDCs, this deposit was the only one present on Mt Ruapehu. However, only ring plain deposits were considered during this study, which means that other deposits were likely overlooked, especially as the focus of the study was to investigate magmatic processes triggering eruptions rather than to identify PDC deposits.

In more recent studies completed by Pardo et al. in 2012 and 2014, further PDCs were hypothesised based on evidence of collapsing eruption columns in the ashfall record. One event, part of the Oruamatua Eruptive Unit (between 13-12 ka) was found up to 16 km from the source (North Crater) (Pardo et al. 2014). Another PDC was found in the Okupata-Pourahu Eruptive Unit (11.6 ka) and was found up to 16 km from the source, now the South Crater, which is still active today. PDCs were also identified in the Upper Waikato drainages, most likely formed due to the partial collapse of an unsteady eruption column (Pardo 2012; Pardo et al. 2012a).

The most recent study conducted by Cowlyn (2016) identified 12 previously unknown PDC units on the eastern flank of Mt Ruapehu, drawing attention to, and improving, the current knowledge on a formerly unquantified hazard on Mt Ruapehu. Field identification of PDC deposits was relied upon in this study. The accuracy of these identifications was improved through the use of a confidence-based method created by Cowlyn (2016). This method involves the recognition of certain textural criteria that had been assigned to specific volcanic hazards based on the likelihood of their occurrence. This allowed volcanic deposits not displaying the textural characteristics of a PDC deposit to be disregarded using a ranking system. The PDCs identified by Cowlyn (2016) were determined to have formed from a range of different eruptive styles, from Plinian eruptions to smaller eruptions caused by the collapse of cinders on the steeper slopes. Identified deposits included pumice-rich PDCs, welded scoria-rich PDCs,

and small-volume PDCs. The pumice-dominated PDC deposits often travelled further than other deposits and were found to be geochemically similar to nearby Plinian fall deposits. This eruption and PDC style was also seen at Mt Pinatubo during the 1991 eruption (Pardo et al. 2012a). The scoria-dominated, welded deposits had more silicic pyroclasts and only occur in the proximal area of the volcano. These deposits were interpreted to have formed from the gravitational collapse of accumulated spatter near to the vent or sustained strombolian fountaining, similar to deposits seen at Santorini and Summer Coon volcano, Colorado (Mellors & Sparks 1991; Valentine et al. 2000). The young, small-volume PDC deposits are characterised by 'cauliflower' and 'breadcrust' bombs. These deposits have a limited distribution and have been interpreted as being formed during smaller sub-plinian or Vulcanian eruptions due to a lack of associated tephras. Similar PDCs were also generated during the 1975 Ngauruhoe eruption (Nairn & Self 1978; Lube et al. 2007).

**Figure 4. The 1945 eruption at Mt Ruapehu (Johnston & Neall 1995) with an apparent PDC flowing down the slope and on the right. Based on the location the PDC likely flowed into the Wahianoa Valley, which was not visited during this study.**

Overall, few studies have mentioned PDCs on Mt Ruapehu. While Cowlyn (2016) identified some deposits on one side of Mt Ruapehu, there is still a significant gap in the knowledge of the occurrence of PDCs on this volcano. Therefore, it is important to improve awareness on the hazard proposed by Cowlyn (2016) and to determine past PDC occurrence over the entire volcano.

# 2. Methods

## 2.1 Field work

Field work formed the basis of this study, where a total of three months of field work was conducted on Mt Ruapehu between November 2017 and March 2018. Potential locations to investigate were based on previous visits of other scientists (Figure 5).

Each location was visited and assessed systematically. This involved the sampling, identification, and description of potential PDC deposits using a confidence-based method developed by Cowlyn (2016) (Figure 6).
Contextual observations of the surrounding landscape and units were made to support the findings of this chart. For example, outcrops found near to tops of ridges far from the source, were determined as being more likely to have originated from a PDC.

At each deposit the outcrop size and thickness was measured. It was described with textural observations, including colour, grain size, roundness, vesicularity, preservation, sorting, and grading. Nearby units were recorded to assist with stratigraphic correlation of the outcrop and age estimates.

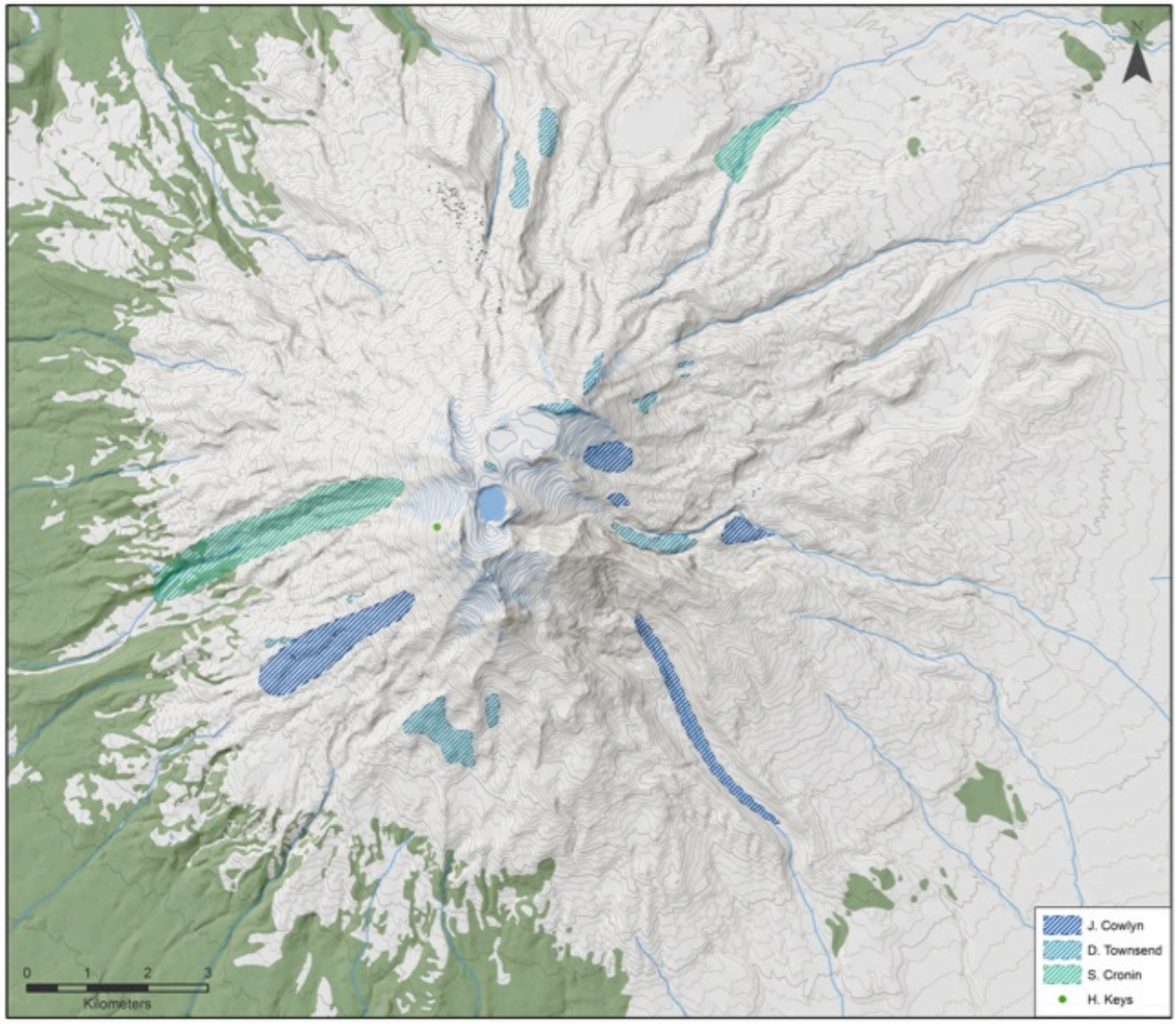


**Figure 5. Potential PDC locations, suggested by other researchers and those familiar with the region, that were investigated in this study. Note the Wahianoa Valley deposit (south-east side of Mt Ruapehu) is the likely path of the 1945 PDC. However, due to time constraints and difficult terrain, this valley was not visited during this project.**

Unconsolidated outcrops were sampled using a small trowel to collect a representative portion of the deposit. Indurated deposits were sampled using a rock hammer, or where very well indurated, a hammer and chisel. This allowed a more precise selection of the outcrop, and a larger sample to be gathered. The hammer and chisel also reduced the amount of damage done to the sample during collection. Sample sizes ranged between 100g and 2kg depending on the

size of the outcrop and how easily samples were able to be taken. The size and quantity of samples were also limited by permit requirements issued by the Department of Conservation. This limited sample size meant that the amount of material had to be divided between the different analyses, where only a small amount of suitable lapilli were available for density analysis after others were removed for geochemical analysis.

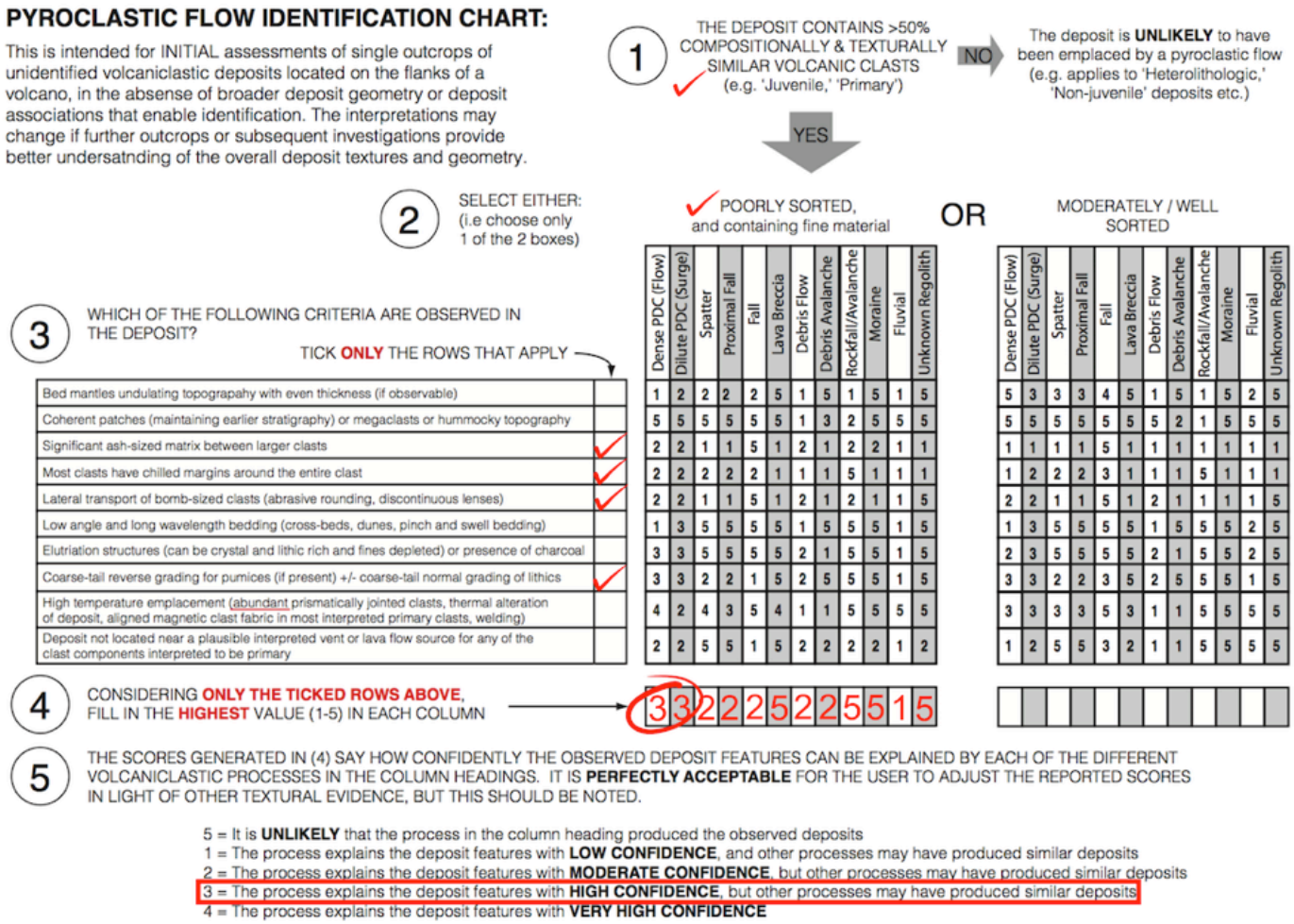


**Figure 6. Worked example of the confidence-based identification chart created by Cowlyn (2016). A pumice-rich deposit was used as an example and was identifed as either a dilute or dense PDC deposit with the same level of confidence (3, high confidence).**

## 2.2 Grain size distribution

The grain size distribution of an outcrop is an important indicator of the type and degree of fragmentation, transport, and deposition it has undergone (Jutzeler et al. 2012). These processes result in varying grain size distributions with different types of volcaniclastic deposits (Walker 1971). Therefore the grain size distribution of unconsolidated deposits found on Mt Ruapehu can be used to differentiate PDC deposits from airfall. Due to the coherent nature of many of the outcrops, only unconsolidated samples were able to be analysed for grain size distribution.

Samples were dried in a 50°C oven for at least 72 hours to ensure they were completely dry. Unconsolidated samples were then dry sieved at a range from -6Φ to 5Φ. Clasts between -6Φ and 0Φ were sieved by hand to prevent the reduction in grain size through breakage. The remaining particles between 1Φ and 5Φ were placed in a mechanical shaker for 5 minutes, as the grain size was too small to efficiently sieve by hand. Each grain size category was weighed, and the weight percentage of each was calculated against the bulk dry weight measured after oven drying.

## 2.3 Density analysis

Representative clasts from each sample were chosen to measure the density of the clasts within each flow. Where the sample size allowed, three clasts were chosen from each. However, due to permit restrictions, some samples were too small and did not contain enough suitable lapilli clasts. In these samples only one representative clast was chosen. To reduce the influence of varying densities with different clast sizes, clasts of similar sizes were chosen where possible. Sizes ranged from medium to coarse lapilli, where the minimum clast size chosen was 17 mm, and the largest 58 mm. After selection each clast was cleaned of excess fine particles and weighed while completely dry.

Using methods described by Houghton and Wilson (1989), the clasts were measured in air and water (Archimede's Principle) to determine the density. To prevent an influx of water into vesicles each clast was wrapped in a consistent quantity of Parafilm wax. The Parafilm sheets were moulded into surface irregularities in the clasts and across vesicles in order to accurately preserve their buoyancy. While all efforts were made to prevent it, it is important to note that due to the irregularity of the surfaces, small air bubbles remained in many samples. This may cause a slight increase in the buoyancy of these clasts, though this error was calculated as not significant (Cowlyn 2016). Due to the coarse surface of many of the clasts and the delicacy of the Parafilm, small tears in the wax were often produced during wrapping. These were sealed with a silicon sealant spray.

The clasts were placed a bucket of deionised water in a cage that was hanging from a zeroed precision balance (Figure 7). The cage prevented buoyant clasts from floating upwards and measured their negative weight. Heavier clasts sank to the bottom of the cage.

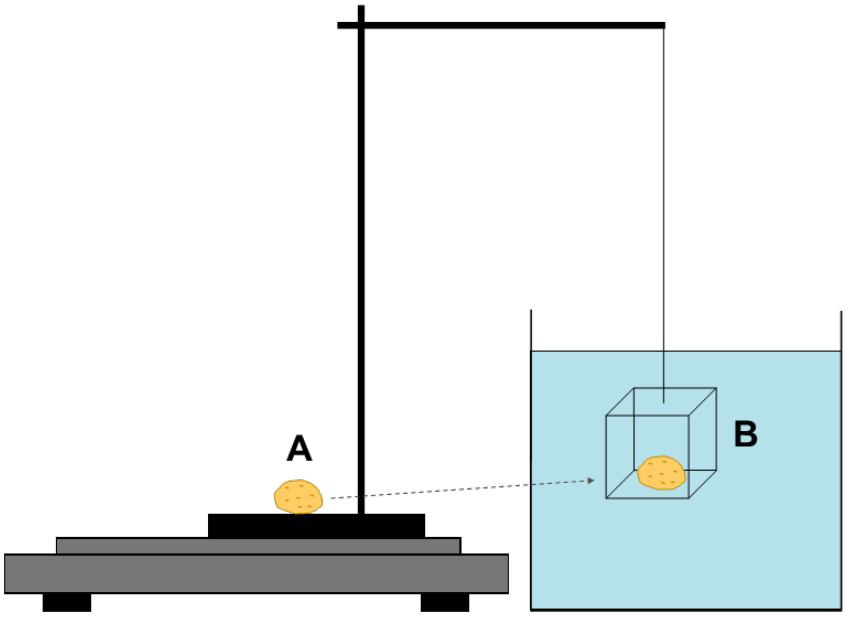


Figure 7. Density analysis process. A) Dry weight of the unwrapped clast measured on a precision balance. B) Wrapped clast placed in cage and the wet weight is measured while the clast is submerged. The enclosed cage prevents some clasts from floating upwards, and allows the buoyancy to be measured.

The density of the clasts were calculated using the equation outlined in Houghton and Wilson (1989) and Cowlyn (2016):

$$\rho_{clast} = \frac{W_{clast(dry)}}{S.G\left[W_{clast(dry)} + W_{wax(wet)} + W_{cage(wet)} - W_{clast+wax+cage(wet)}\right]}$$

Where $W_{clast(dry)}$ is the weight of the clast measured while dry, $S.G$ is the specific gravity of water, and $W_{cage(wet)}$ the weight of the cage while in water. $W_{wax(wet)}$ is the weight of the wax while being held underwater in the cage. The buoyancy of the wax resulted in a negative value.

Note: the S.G. of water varied depending on its temperature, and changed daily. This has been accounted for in the equations for each individual clast.

## 2.4 Vesicularity

To create thin sections of the samples, a representative clast from each sample was chosen. If the clast was large enough, the weathering rind was removed using a rock saw. The clasts were then cut into rectangular billets and were used to create a thin section.

The thin sections were analysed under a transmitted light microscope and the vesicularity percentage was estimated by comparing the amount of vesicles against a typical grain size percentage chart. This method was used consistantly on all samples to create comparable results.

## 2.5 Geochemistry

The geochemical analysis of samples is a crucial component of this study as the data are used to correlate deposits with known geochemistry of past eruption deposits. Previous studies at Mt Ruapehu report both major and trace element

XRF results, though the most comprehensive data set is major element whole rock XRF data (Pardo 2012; Conway et al. 2016; Cowlyn 2016; Townsend et al. 2017). For this reason we decided to focus on whole rock major element geochemistry. A geochemical correlation combined with stratigraphic field relationships allows an estimated age for each deposit to be determined. Geochemistry also allows deposits from the same eruption to be correlated.
Where possible, on large clasts the weathering rind was cut off prior to processing. Cleaned and dried samples were crushed first in a disc mill to reduce the grain size, then in a ring mill to produce powders for analysis. Powders were dried in a 100°C oven overnight.

To prepare the samples, 2g of dried powders was measured and placed in a Muffle Furnace at 900°C for 3 hours in order to burn off organic material. The powder was weighed prior to and after being placed in the furnace in order to calculate the LOI. To create glass beads for analysis, 0.8g of sample material was mixed with 8g of X-Ray Flux (35.3% Lithium Tetraborate, 64.7% Lithium Metraborate).

The geochemical analyses were conducted at Massey University using a Bruker S8 TIGER Series 2 WDXRF Spectrometer calibrated against certified international standards (OREAS 24c).

Due to technical issues, the trace element data was unable to be obtained.

### 2.6 Flow paths and volume estimates

The flow extent of deposits was extrapolated based on the thickness of each deposit, an estimation of palaeotopography, and the flow type, following the methodology outlined by Cowlyn (2016). The topography was also used to help influence the shape of PDC deposits assuming glaciers covered topography higher on the flanks, thus reducing the topographic influence on deposition. At

middle distances the steep incised channels would help to confine the flows, whereas further from the summit the flows would spread as channels become shallower.

Volume calculations for each flow were made using the average thickness measured in outcrop at each deposit and the visible exposed area of the deposit. A second volume calculation was made by extrapolating the area of the flow based on the estimated flow path compared to similar pyroclastic flow types in Cowlyn (2016).

Determining flow paths and volumes of PDC deposits is difficult to do with any accuracy as erosion has removed many outcrops and reduced the original thickness. Therefore, it is important to note that the flow paths and volumes given by both these methods are minimum values.

### 2.7 PDC ages

Most of these deposits were not texturally appropriate to date radiometrically as was done with lava flows (Conway et al. 2016). Therefore, the ages of PDCs were estimated by geochemically correlating deposits with known units that have ages associated with them (Pardo 2012; Conway et al. 2016). This was also confirmed by comparing the relative stratigraphy of the PDCs to the surrounding units on a geological map of Mt Ruapehu (Townsend et al. 2017). Where PDCs were stratigraphically overlying the dated units on the map, it was determined that they were younger than the age of that unit. This technique allowed the age of the PDC deposits to be approximately bracketed.

# 3. Results

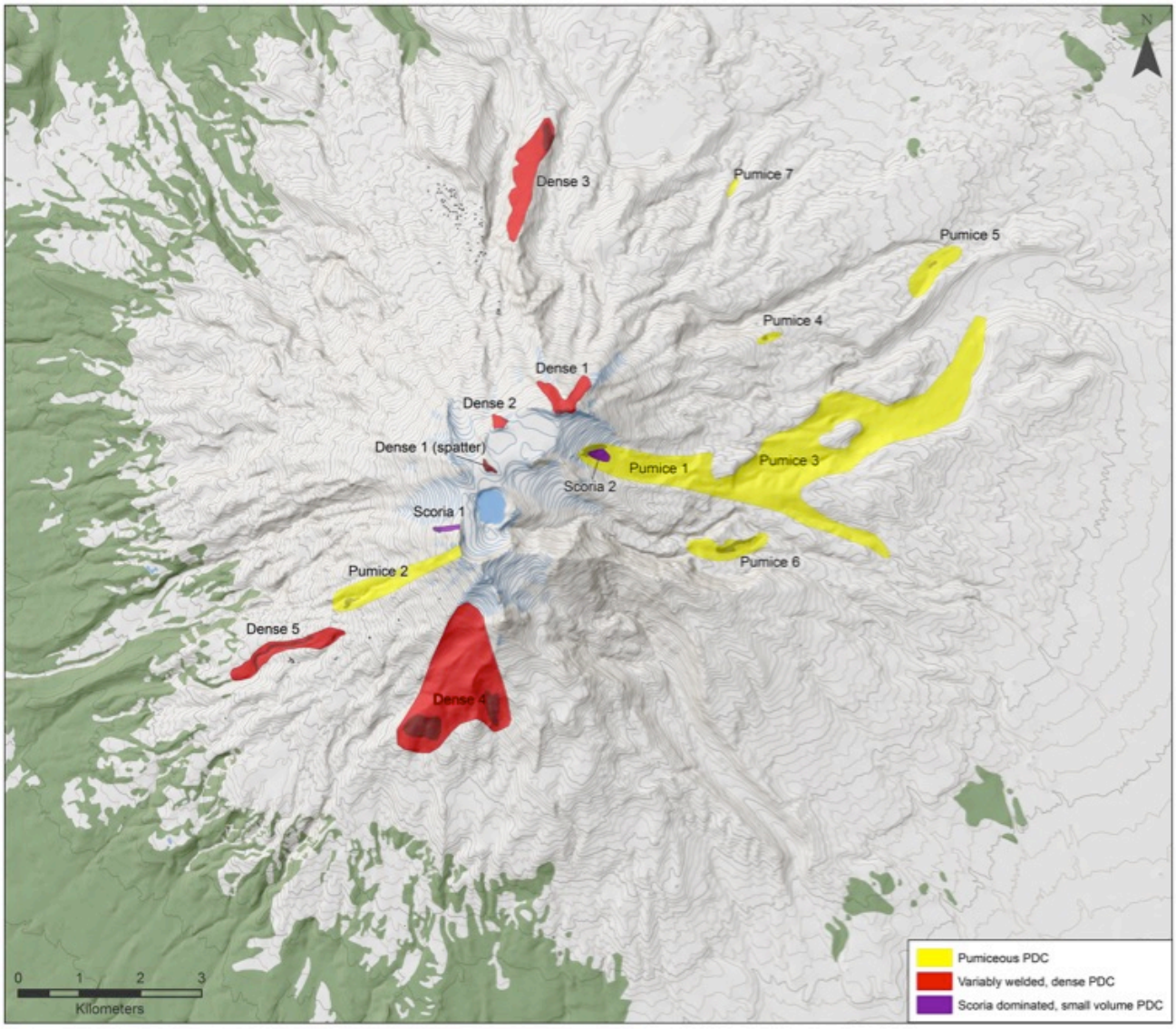


**Figure 8. PDCs and flow paths identified during this study. Darker areas represent the deposits seen in the field. Larger areas are extrapolated flow paths based on the deposits. A total of 14 PDCs were identified.**

## 3.1 PDC categories

A total of 14 pyroclastic density current deposits were identified on Mt Ruapehu on the northern, eastern and south-western sectors of the mountain (Figure 8). These PDC deposits have been categorised into three main groups based on textural characteristics, geochemistry and previous work by Cowlyn (2016):

- Pumiceous PDC
- Variably welded, dense PDC
- Scoria-dominated, small volume PDC

These textural groups correspond with the groups identifed by Cowlyn (2016)– pumice-dominated PDC; scoria-dominated variably welded PDC; and heterogeneous, small volume PDC, respectively.

For the purposes of this report, the term “pumiceous” is used as a textural description of porosity greater than 50% rather than compositional, as all of the samples are within the range of basaltic andesite to andesite. “Scoriaceous” is used to describe clasts with porosity less than 50%.

### *3.1.1 Pumiceous PDC*

The pumiceous PDC textural group encompasses pumice-dominated deposits that are typically a pale brown colour, matrix supported, and poorly sorted. This category includes both andesitic and basaltic andesite PDCs. A total of seven flows (50%) were found. Some instances of this deposit type are only a few centimetres thick and are generally surrounded by ashfall layers (Figure 9A). These deposits range from fine ash to moderate lapilli. Other deposits in this group were thicker, reaching up to 6 m; with large, up to 1 m, cauliflower bombs making up 25% of the deposit (Figure 9B). The density of the clasts in these deposits is generally low, ranging from 0.83-1.31 g/cm$^3$. This corresponds with a generally moderate to high vesicularity, with values ranging from 50-60% (Figure 10). Most deposits also contain small, denser lithic fragments. While the majority of deposits in this category are poorly indurated, two deposits found were well indurated, with some minor reverse grading (Figure 9E). Both are comprised of an orange matrix with dark grey or black scoriaceous bombs (Figure 9F). Well-rounded and less vesicular lithics occur in this group, though they only account for approximately 5% of the clasts in these outcrops. While these deposits are well indurated, they are included in this group due to the flow length (4-7 km),

thickness (1-5 m), and the clasts with 50-60% vesicularity. These characteristics are consistent with others in this textural category.

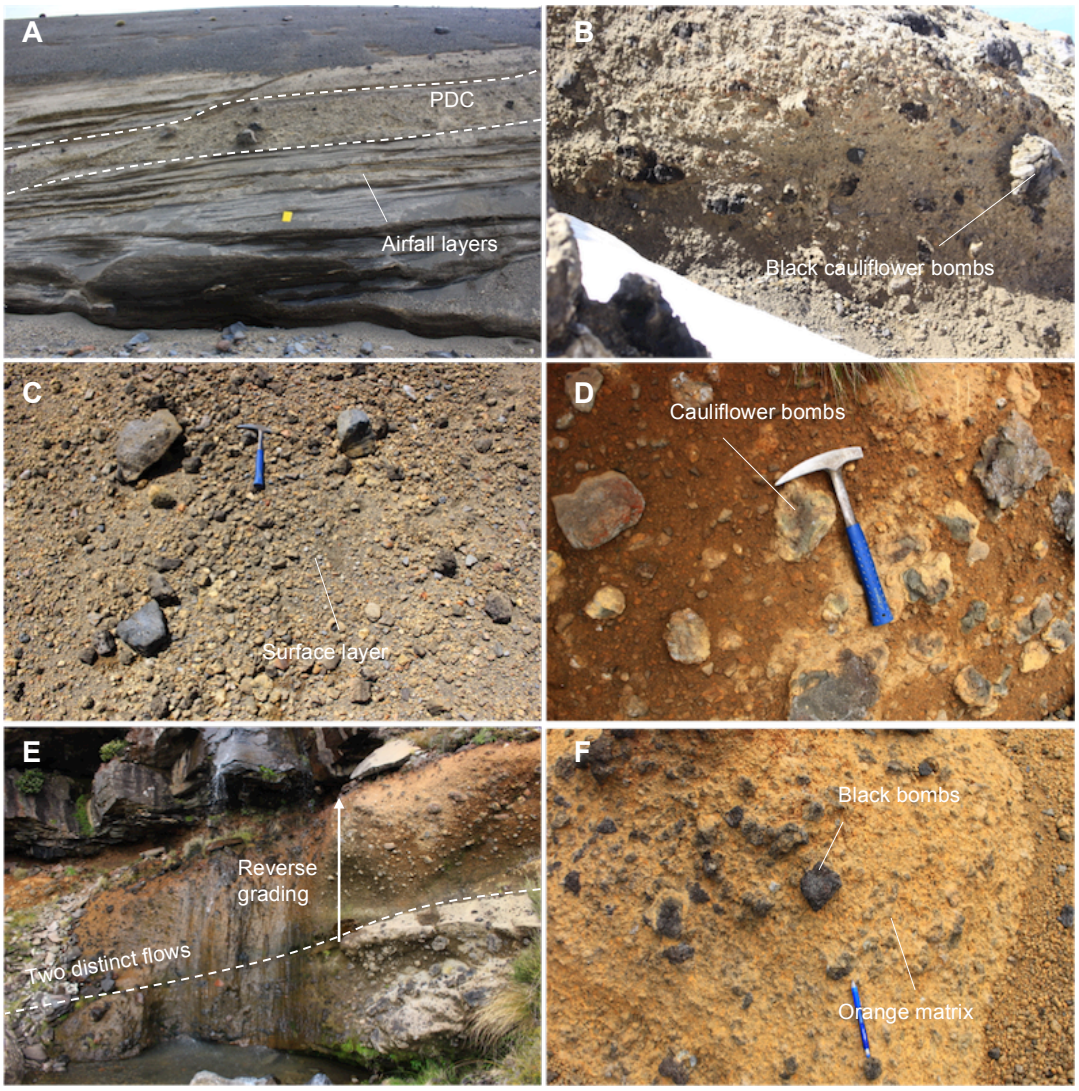


**Figure 9. Pumiceous PDC end members. A) PDC bounded by airfall layers. B) Thick poorly indurated PDC with black bombs. C) Poorly indurated surface veneer. D) Well indurated PDC with cauliflower bombs. E) Thick, well indurated deposit displaying minor reverse grading in upper flow. F) Well indurated deposit with orange matrix and black bombs.**

Based on the confidence-based PDC identification methodology developed by Cowlyn (2016) (Figure 6), most of these deposits have been identified as PDCs with “moderate confidence” (confidence level 2). This is based

on the poor sorting, ash matrix, and rounded clasts. One deposit that also displayed reverse grading was identified with “high confidence” (confidence level 3). The two indurated deposits were determined to be PDCs with “very high confidence” (confidence level 4). This is based on the presence of minor reverse grading in the outcrops, chilled margins, and prismatic jointed and bread-crusted clasts, suggesting high temperature emplacement (Benage et al. 2014) (Figure 9D).

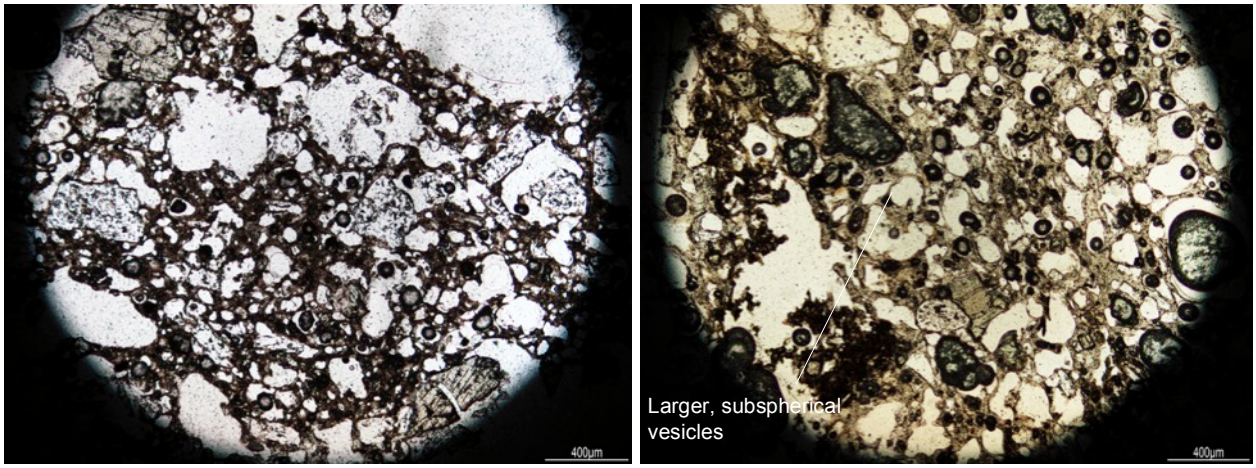


**Figure 10. Examples of the pumiceous PDC vesicularity. Smooth, subspherical vesicles are predominant.**

This deposit type was primarily found on the eastern side of Mt Ruapehu, with one deposit found on the south-western side, and another found on the northern slopes. The deposit found furthest from the source was located over 9 km away from the crater. Other outcrops were found as close as 2 km from the current vent (Figure 8). The areas of each deposit ranged from 0.000346-0.041 $km^2$, with volumes between 0.2-23 $x10^{-5}$ $km^3$.

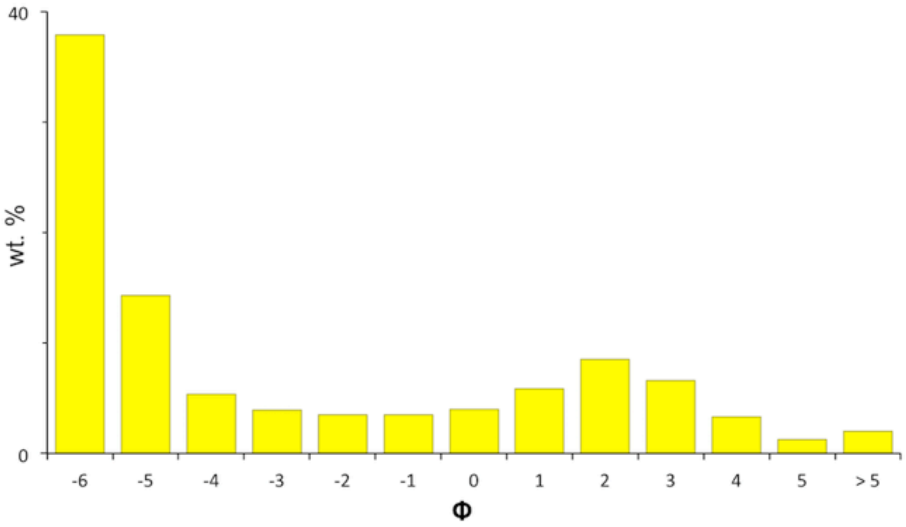


**Figure 11. Grain size distribution of a typical pumiceous PDC deposit. There is a slight bimodal distribution, with a peak in wt. % at larger grain sizes, then a small peak at grain sizes between 1-2 *Φ*. For other unconsolidated deposit grain size distributions see Appendix 1.**

The grain size distribution of the poorly indurated deposits shows a trend of decreasing weight percent with decreasing grain size. The majority of each sample's weight is composed of clasts around 6 to 5*Φ*. Many of the distributions show a small peak at approximately 1 to 2*Φ* (Figure 11).

### *3.1.2 Variably-welded, dense PDC*

The PDC deposits that occur in this group differ significantly from the pumiceous PDC textural group as they are well indurated outcrops and have clasts with marginally higher densities ranging from 1.32-1.58 g/cm$^3$ (Figure 12), and vesicularities between 1-30% (Figure 13).

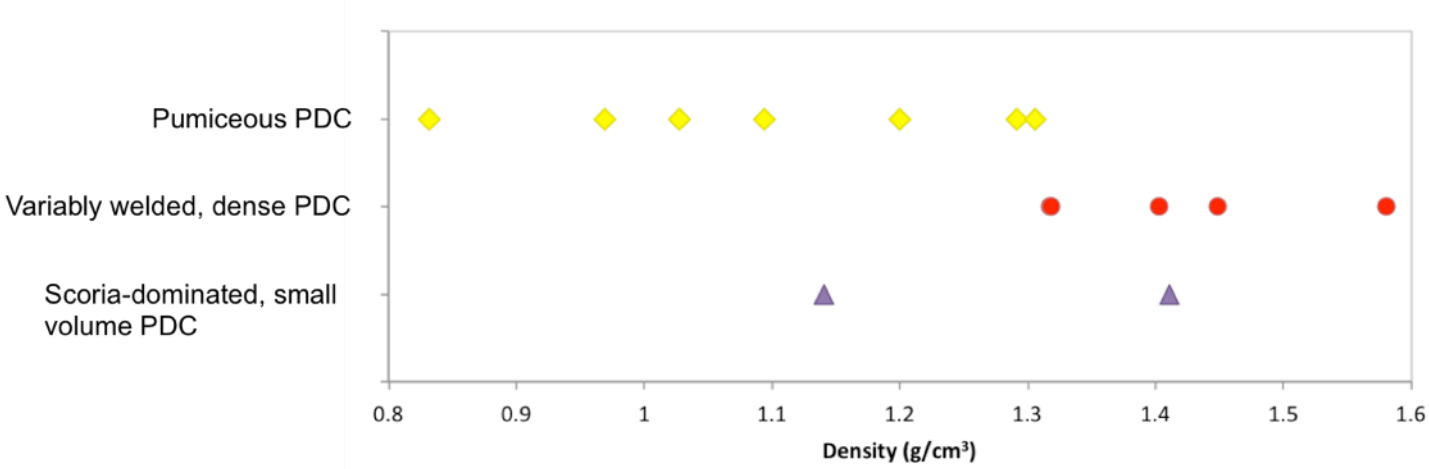


**Figure 12. Average density results of all PDC deposits. Pumiceous PDCs have the lowest density (0.83-1.31 g/cm$^3$), variably welded, dense PDCs have the highest densities (1.32-1.58 g/cm$^3$), scoria-dominated, small volume PDCs have a moderate density (1.14-1.41 g/cm$^3$). For raw density data see Appendix 2.**

Five (36%) flows were identified as being part of this group. Most outcrops have distinct pink or red colouration throughout the entire outcrop or in isolated patches (Figure 14A-B). The remaining outcrops were light to dark grey. Outcrops of this group had thicknesses varying from 1 m up to approximately 15 m. These thicknesses are only the visible outcrop thicknesses, and it is important to consider that the deposit may have reached greater thicknesses prior to erosion. In the field most outcrops were a distinct unit with loose material of the same composition on top, indicating a varying degree of welding during deposition (Figure 14A). Overall, this textural group is typically poorly sorted, contains sub-rounded clasts, and is matrix supported, though containing a significant proportion of clasts–up to 30% of the outcrop. Clasts sizes are between 30-50 cm in most of the outcrops in this group.

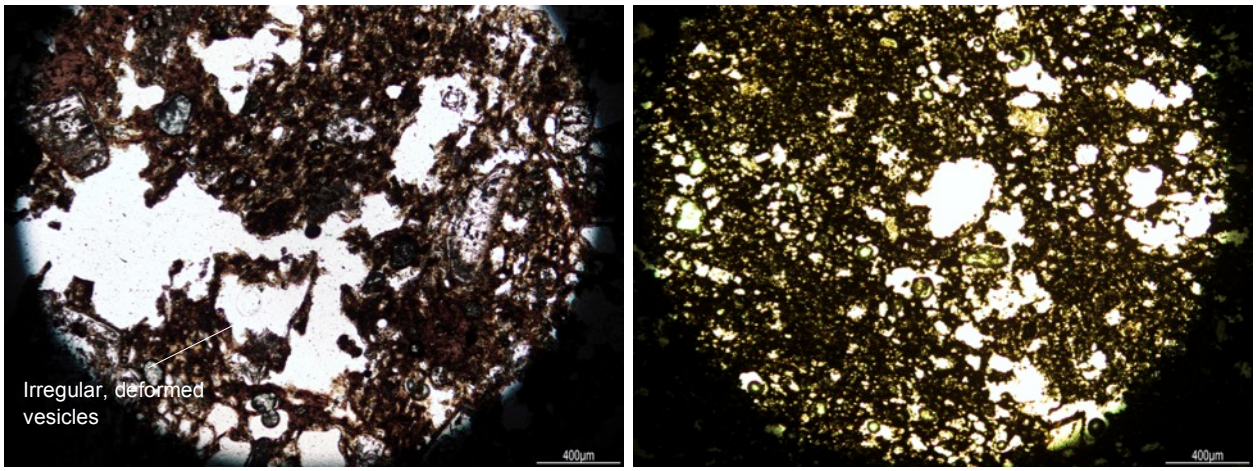


**Figure 13. Vesicularity images of the dense, variably welded PDC group. Vesicles have been deformed and are now rough and irregular.**

In some outcrops a spatter-like component was incorporated, often at the top of the unit or in distinct layers within it. (Figure 14D). Where there is this fluidal texture the clasts and matrix are nearly indistinguishable in texture and hardness. In many of the other outcrops where the clasts are distinct from the matrix, the ash matrix is significantly softer than the clasts and can easily be scratched with a hammer, whereas the clasts are unmarked when scraped.

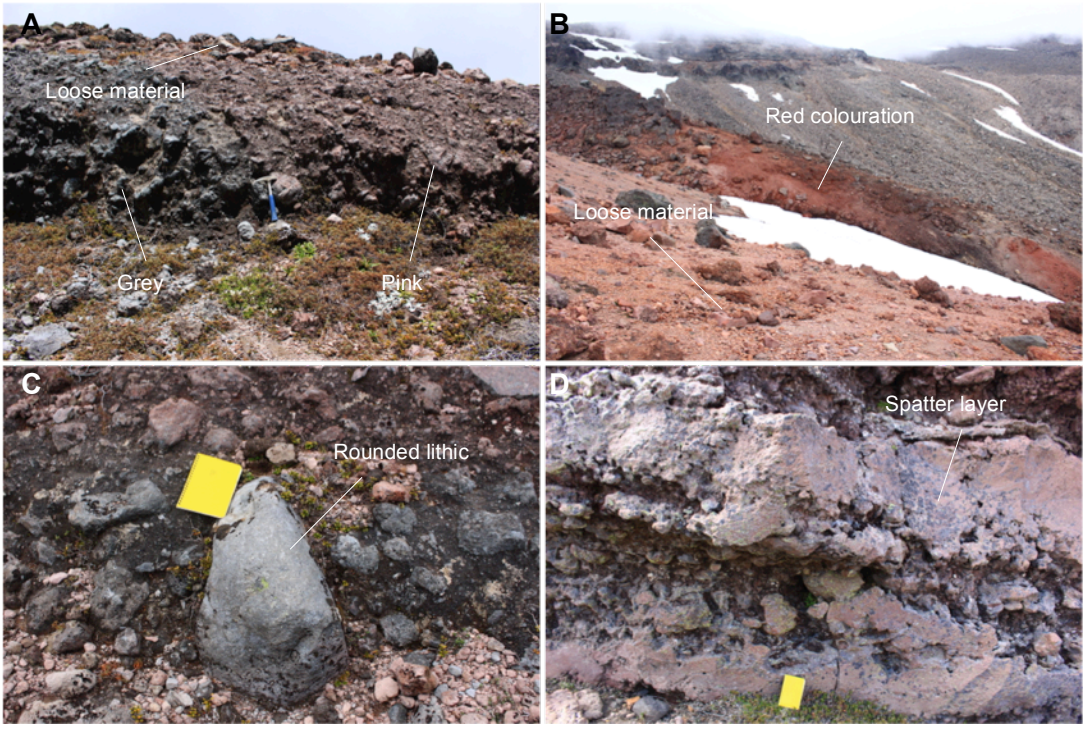


**Figure 14. Typical dense, variably welded PDC outcrops. A-B) Well indurated deposits with loose material on top indicating variable welding. Both also have varying red/pink and grey colouration. C) Large, well rounded lithic clast within PDC deposit. D) Large, discontinuous spatter-like layers within PDC flow. Only seen in some parts of the outcrop.**

Using the confidence-based PDC identification chart, these outcrops were identified as PDCs with "very high confidence" (confidence level 4). This identification is based on the red thermal alteration seen in all of the deposits as it is evidence of high-temperature emplacement, which eliminates the possibility of lahar or debris avalanche deposits. However, due to this high temperature emplacement alteration, lava breccia and spatter were also identified with "very high confidence".

This deposit type was found on the north, north-eastern, and south-western slopes of Mt Ruapehu. The furthest outcrop from the modern-day vent was found over 6km away. The deposit areas ranged between 0.047-0.286 $km^2$, with the volumes ranging between 8.7-110 $x10^{-5}$ $km^3$.

### *3.1.3 Scoria-dominated, small volume PDC*

The scoria-dominated PDC textural group is characterised by black scoriaceous outcrops, with small apparent run-out distances. Two (14%) PDCs were identified from 14 outcrops. This group differs from the previous PDC group as the texture is primarily moderately vesicular, glassy scoria rather than denser juvenile clasts. These outcrops are typically poorly sorted, poorly to moderately indurated, monomictic, contain sub-rounded clasts, and are generally matrix supported, containing 30% clasts (Figure 15A). However, one deposit in this group was identified as clast supported with up to 50-60% clasts. The maximum clast size seen in this group is 50 cm. In some instances, the appearance of sub-rounded clasts may be a result of thermal expansion during the formation of these clasts rather than abrasion during transport. This is confirmed by the occurrence of bread-crust texture and glassy chilled margins on clasts in some of the outcrops. The density of the clasts was moderate ranging from 1.14-1.41 $g/cm^3$ (Figure 12). The vesicularity was correspondingly moderate, with values between 40-45% (Figure 14C).

These deposits were identified as PDCs with “moderate” or “very high confidence” (confidence level 2 or 4). This is based on the evidence of high temperature emplacement in the form of bread-crust and cauliflower texture (Figure 15B), thermal alteration and chilled margins. Where there was no evidence of high temperature in one of the outcrops in this group, it could only be assigned with “moderate confidence”.

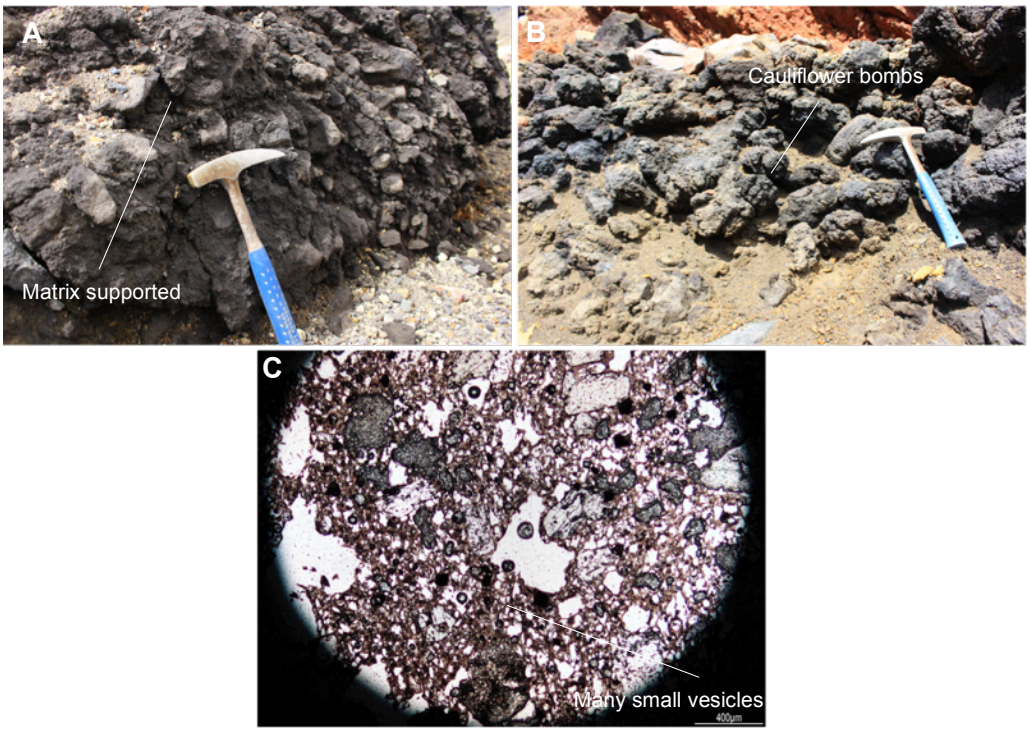


**Figure 15. Typical scoria-dominated, small volume PDC outcrops. A) Well indurated deposit (Scoria 2). B) Poorly indurated deposit with fines winnowed away (Scoria 1). C) Representative vesicularity of PDC textural group. Small, subspherical vesicles are most common.**

The deposits in this group are generally smaller, found at the edges of the North and South Crater, with the furthest deposit only being found 2 km from the vent and the thickest reaching only 2 m. The deposit areas range between 0.0021-0.0029 $km^2$, and the volumes between 0.3-0.6 $x10^{-5}$ $km^3$.

## 3.2 Geochemistry

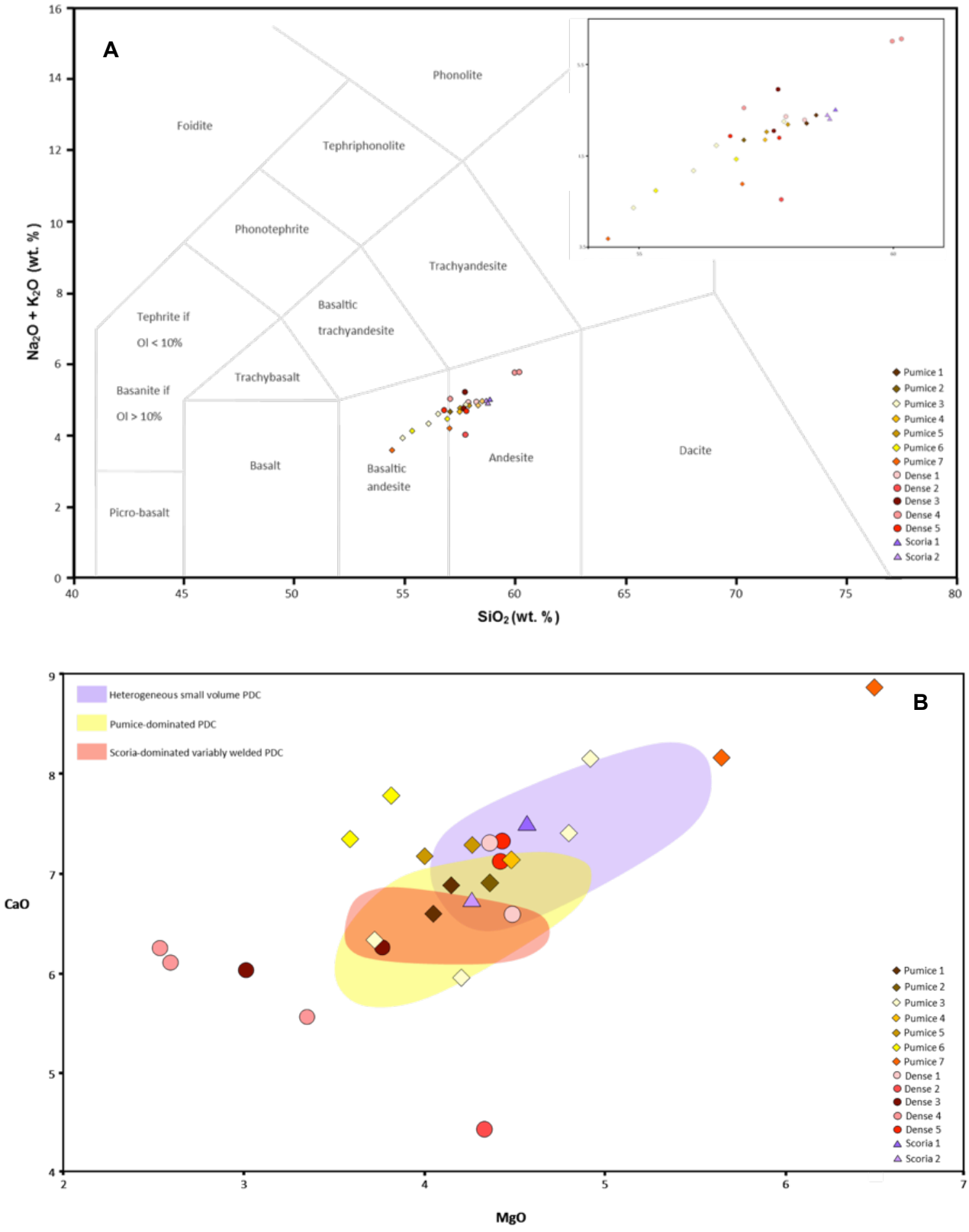


Figure 16. Major element results from geochemical analyses. A) TAS with inset showing a closer view of the geochemical distribution of deposits. B) MgO/CaO diagram comparing the PDCs identified by Cowlyn (2016) with those from this study. For raw geochemistry data, see Appendix 3.

We show the TAS diagram for classification purposes and follow Cowlyn (2016) by plotting CaO/MgO to distinguish different PDC types. The comparison of different flows using the MgO/CaO diagram will be later discussed in Section 4.2.

Figure 16A shows that all deposits fall within the basaltic andesite to andesite geochemical range. The pumiceous PDC group plots at 54.38-58.48 wt% $SiO_2$, the dense, variably welded group plots at 56.18-60.16 wt % $SiO_2$, and the scoria-dominated, small volume group plots at 58.69-58.85 wt% $SiO_2$. Both the pumiceous PDC group and the variably welded, dense group have the largest compositional range and the scoria-dominated group has a very small range.

Figure 16B plots the textural groups as large, overlapping clusters. The pumiceous PDC group contains the highest MgO/CaO values and plot at 3.58-6.5 wt% MgO. This group has a greater range than the pumice dominated PDC group identified by Cowlyn (2016). The dense, variably welded group contains the lowest MgO/CaO values, though it overlaps with the pumiceous group, and plots at 2.52-4.82 wt% MgO. The variably welded group identified by Cowlyn (2016) falls within the range of the equivalent textural group from this study. The scoria-dominated, small volume group overlaps with both other groups and has the smallest range in MgO/CaO values, plotting at 4.25-4.58 wt% MgO. These deposits plot within the range of the small volume PDC group identified by Cowlyn (2016). While the distribution of textural groups does not correspond exactly with those identified by Cowlyn (2016) both variably welded groups contained the lowest MgO/CaO values, with the pumiceous PDC groups plotted above. This suggests a similar overall distribution in this study as what was seen in Cowlyn (2016). This graph will be used in Section 4.2 to help correlate the PDCs identified in this study with the PDCs and eruption styles identified by Cowlyn (2016).

As the geochemistry of the units forming Mt Ruapehu do not evolve linearly over time (Townsend et al. 2017), it is difficult to solely use the $SiO_2$ content of the deposits to determine relative ages. Therefore, the deposit geochemistry will be compared with other studies to help correlate the deposits with known eruptive periods.

Overall, the compositional range of the samples gathered is relatively small, with only 4wt% $SiO_2$ separating the lowest and highest sample. This lack of variation will lead to difficulties distinguishing units and eruptive periods based on compositional differences.

### 3.3 Volume estimates

| | Deposits | | | Estimated flow paths | | |
|---|---|---|---|---|---|---|
| | Thickness (m) | Area ($km^2$) | Volume ($x10^{-5}$ $km^3$) | Area ($km^2$) | Volume ($x10^{-5}$ $km^3$) | Aspect ratio (H/L) (m/km) |
| Pumice 1 | 7 | 0.0324 | 23 | 1.13 | 790 | 1.7 |
| Pumice 2 | 1 | 0.0159 | 1.6 | 0.62 | 62 | 0.33 |
| Pumice 3 | 1.5 | 0.0009 | 0.1 | 4.21 | 630 | 0.17 |
| Pumice 4 | 1 | 0.0046 | 0.5 | 0.041 | 4.1 | 0.18 |
| Pumice 5 | 1.3 | 0.0055 | 0.7 | 0.31 | 41 | 0.14 |
| Pumice 6 | 0.9 | 0.0407 | 3.7 | 0.34 | 31 | 0.23 |
| Pumice 7 | 5 | 0.0003 | 0.2 | 0.027 | 14 | 0.91 |
| Dense 1 | 2 | 0.0105 | 2.1 | 0.23 | 46 | 0.77 |
| Dense 2 | 5 | 0.0375 | 19 | 0.038 | 19 | 3.33 |
| Dense 3 | 1.5 | 0.0579 | 8.7 | 0.61 | 91 | 0.5 |
| Dense 4 | 4 | 0.2857 | 110 | 2.47 | 990 | 0.8 |
| Dense 5 | 3 | 0.0471 | 14 | 0.41 | 120 | 0.5 |
| Scoria 1 | 1.5 | 0.0021 | 0.3 | 0.28 | 2.8 | 1.5 |
| Scoria 2 | 2 | 0.0029 | 0.6 | 0.066 | 13 | 1 |

**Table 1. Rounded volume estimates for PDC deposits and extrapolated flow paths. Aspect ratio calculation is of thickness of the deposit (H) divided by the flow path length (L). Overall, the pumiceous PDC and dense, variably welded PDC groups contain the highest volume values.**

The volume estimates show that the largest deposits and estimated flow paths occur in the pumiceous PDC and variably welded, dense PDC groups. The average volumes of these two groups are 225 $x10^{-5}$ $km^3$ and 250 $x10^{-5}$ $km^3$, respectively. Whereas the average volume of the scoria-dominated, small volume PDC group is only 8 $x10^{-5}$ $km^3$.

### 3.4 Summary

| | Confidence level | Density ($g/cm^3$) | Vesicularity (%) | $SiO_2$ (wt %) | MgO (wt %) | Field characteristics |
|---|---|---|---|---|---|---|
| Pumiceous PDC | 2-4 | 0.83-1.31 | 50-60 | 54.38-58.48 | 3.58-6.5 | Pumice-rich, light brown outcrops. Poorly sorted, matrix supported, fine ash matrix with lapilli and bomb clasts. Occasional cauliflower and breadcrusted bombs, and minor reverse grading. Sub-rounded clasts. |
| Variably welded, dense PDC | 4 | 1.32-1.58 | 1-30 | 56.18-60.16 | 2.52-4.82 | Dense, sub-angular to sub-rounded clasts with small vesicles. Matrix supported. Pink/red and grey/black outcrops. Poorly sorted, well indurated, with loose material on top. Fine ash matrix with bomb clasts. Some outcrops contain coherent spatter segments. |
| Scoria dominated, small volume PDC | 2-4 | 1.14-1.41 | 40-45 | 58.69-58.85 | 4.25-4.58 | Poorly sorted, sub-rounded clasts, moderately vesicular. Monomictic, poorly sorted, ash matrix. Breadcrusted and cauliflower bombs. |

Table 2. Summary table of PDC textural groups. For more detailed results of each individual PDC, see Appendix 4.

# 4. Discussion

## 4.1 Stratigraphic ages

In this section the flow types will be separated into the individual deposits, and these will be described and an approximate age assigned using geochemistry and relative stratigraphy. Note that the unit names (e.g. Pumice 1, Scoria 1) indicate the textural group and the stratigraphic order of the deposits within the textural group, where the lower numbers are more recent.

### *4.1.1 Pumiceous PDC*

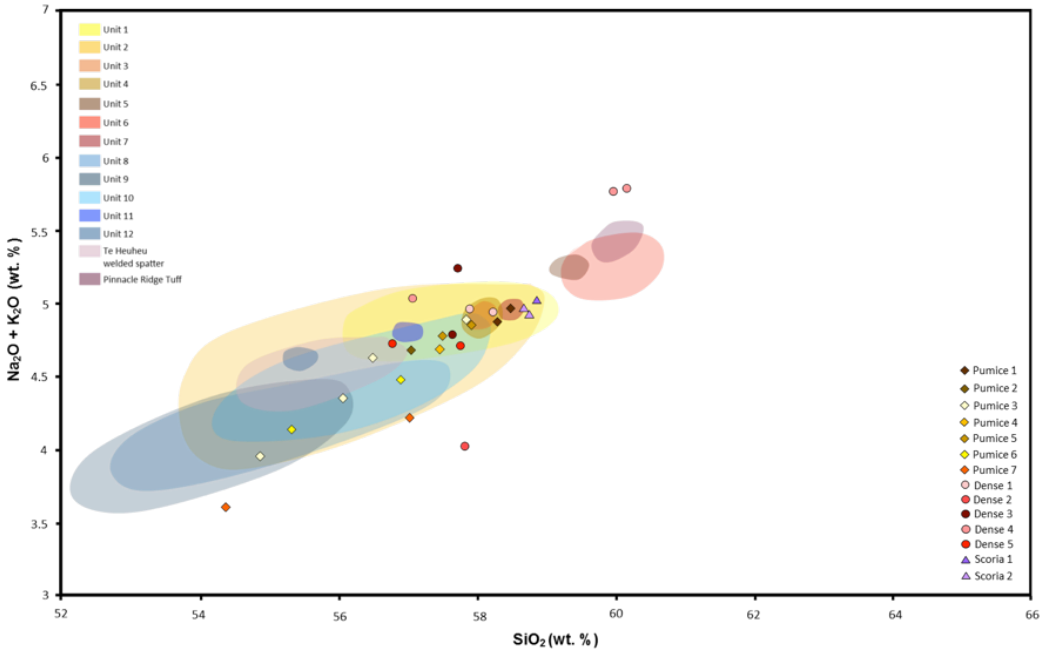


Figure 17. Geochemical TAS diagram comparing Cowlyn (2016) PDC units with this study.

#### *Pumice 1*

This unit is located below the Mangatoetoenui Glacier, outcropping in several places across the valley. Overall, it is a thick unit (~6 m), with pale yellow-grey pumice and large black bombs. Geochemically, it correlates with "Unit 2" identified by Cowlyn (2016) (Figure 17). Texturally it is also similar, however it does not correlate stratigraphically. "Unit 2" was deposited prior to

11.6 ka; however, Pumice 1 has been deposited on top of the Mangatoetoenui lava flows (Iwikau Member), which are dated at 9.2 ± 8.0 ka (Townsend et al. 2017). This suggests that Pumice 1 is a separate PDC than what has been previously identified. Pumice 1 also appears to have been deposited prior to the Tawhainui flows (6.0 ± 2.4 ka) (Conway et al. 2016).

When compared with overall geochemical data of the Ruapehu Group formations, Pumice 1 closely corresponds with the Whakapapa Formation (Figure 18), especially the Iwikau Member (<11.7 ka) (Conway et al. 2016; Townsend et al. 2017). This suggests that the PDC may have occurred during an eruption that contributed to the formation of the Iwikau Member, which coincides with the relative timing based on stratigraphy. Therefore, Pumice 1 was likely deposited between 9.2 ± 8.0 and 6.0 ± 2.4 ka.

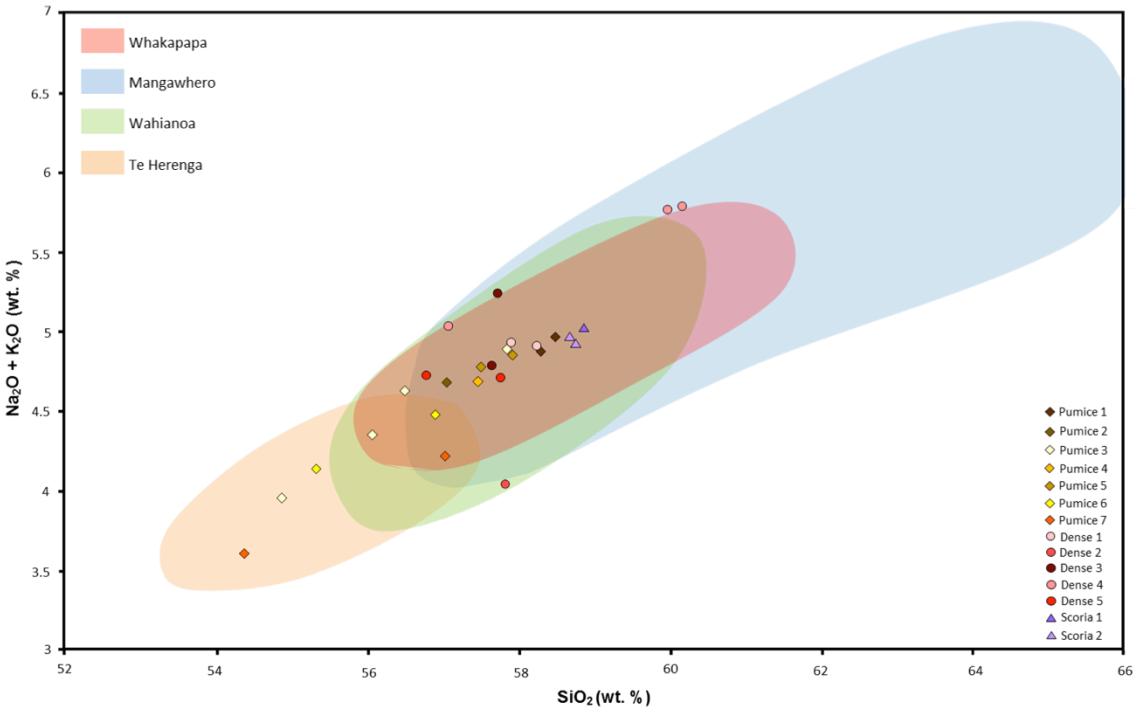


Figure 18. Geochemical TAS diagram comparing Conway et al. (2016) formations with PDCs in this study.

### *Pumice 2*

Pumice 2 was found on the south-western side of Mt Ruapehu as a large, poorly indurated surface outcrop deposited on top of the Turoa Member lava flows (~15-11.7 ka) (Townsend et al. 2017). Geochemically, this unit correlates most with the Mangatoetoenui eruptive sequence (Figure 19) (Pardo 2012). However, the Mangatoetoenui eruptive sequence was identified as being an oscillatory, but non-collapsing eruption column, which suggests that it did not generate Pumice 2 (Pardo et al. 2014).

This deposit also falls within the geochemical range of the Okupata-Pourahu eruptive sequence, which has been identified as having an unsteady eruption column and corresponding PDC deposits (Donoghue et al. 1995; Pardo et al. 2014). This PDC deposit was described as poorly sorted, matrix supported, massive, and containing sub-rounded pumice (Pardo 2012). While the Okupata-Pourahu PDC appears similar to Pumice 2, it is not enough to confirm that they originated from the same eruption, especially as the Pourahu PDC was found on the eastern side of Ruapehu. This may be explained as separate column collapses during the eruption sequence, though that cannot be confirmed.

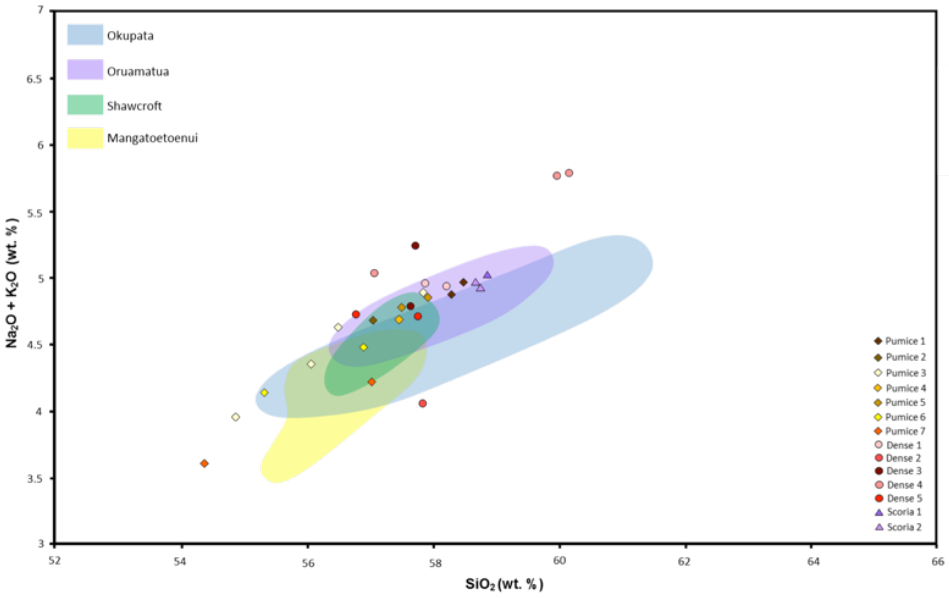


Figure 19. Geochemical TAS comparing Pardo (2012) with this study.

Overall, due to the ambiguity of the geochemistry results, it can only be inferred that Pumice 2 was deposited within the last 11.7 ka, based on the geochemical and stratigraphic information (Pardo 2012; Conway et al. 2016; Townsend et al. 2017).

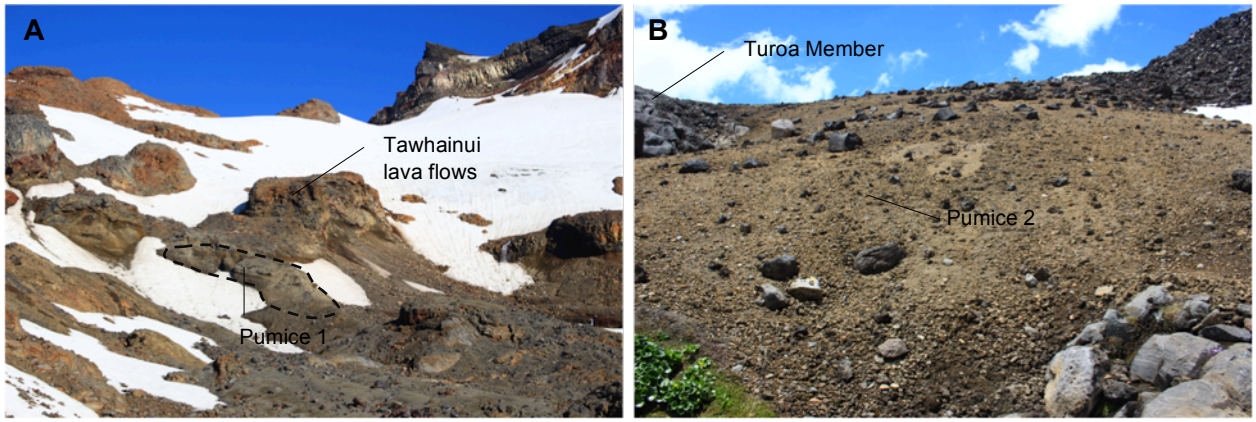


**Figure 20. Outcrop photos showing stratigraphic relationships, A) Pumice 1, with overlying Tawhainui lava flows. B) Pumice 2, overlying Turoa Member lava flows**

### *Pumice 3*

Pumice 3 was found in several locations on the eastern side of Mt Ruapehu primarily as a thin surface veneer.

#### Location 1

This deposit is a thin, well indurated surface veneer. Only 1 m was exposed in this location, and contained a pale ash matrix with black lapilli and bomb clasts. The geochemistry of this deposit does not completely align with the ranges identified by Pardo (2012) (Figure 19), though it is located closest to the Okupata eruptive unit, which has been associated with a PDC (Donoghue et al. 1995; Pardo 2012). Given a more similar geochemistry, this outcrop may instead be associated with the "Unit 2" that Cowlyn (2016) identified (Figure 17). The geochemistry of this flow falls within the range of "Unit 2", and is also stratigraphically similar: located on the surface, above another pumiceous PDC ("Unit 1"). Cowlyn (2016) identified "Unit 2" as occurring during the Oruamatua eruptive sequence as the geochemistry aligned. As previously mentioned, the Oruamatua was also associated with PDCs.

Both the PDC identified here and by Cowlyn (2016) are texturally similar, with yellowish-grey, poorly sorted, sub-rounded clasts, ~50% vesicularity, and containing the occasional bomb. Pumice 3 was found to contain more dense lithics, though this may be a product of studying different localities of the flow. Pumice 3 was also identified within 150 m of the outcrop seen by Cowlyn (2016), further supporting the conclusion that they are the same flow.

### Location 2

This deposit was found adjacent to the Round the Mountain walking track (Figure 20), over 2 km away from Location 1. Though the sample from this location is identified as an andesite rather than basaltic andesite, like Location 1, it still corresponds with the geochemical range of "Unit 2". Texturally, it is also similar as both deposits were identified as containing colour-banded clasts, a feature that was not noted in "Unit 1" (Cowlyn 2016). Location 2 is also identified as a surface outcrop, though poorly indurated, unlike Location 1. The flow path of "Unit 2" inferred by Cowlyn (2016) does not reach Location 2, however, this deposit is found in a small valley, which may have acted as a channel for the PDC if it overtopped its main channel, allowing it to inundate this area.

Overall, this suggests that Pumice 3 was emplaced at a similar time, though subsequent to Pumice 4, between 13.6 and 11.6 ka.


**Figure 21. Outcrop photo of Pumice 3 (Location 2). There is no obvious stratigraphic relationship with other units in this location.**

### *Pumice 4*

This deposit was found on the north-eastern slopes of the mountain, where a small channel has exposed a cross-sectional view. Approximately 1 m was exposed underneath about 6 m of fall deposits. When comparing the geochemistry of this deposit against eruptive units identified by Pardo (2012), overlaps were found between Pumice 4, and the Shawcroft (~13 ka) and Oruamatua (13-12 ka) units (Figure 19). A steady eruptive column produced the Shawcroft unit, whereas the Oruamatua unit contains evidence of an unsteady, collapsing column that produced a PDC (Pardo 2012; Conway et al. 2016).

Texturally both Pumice 4 and the Oruamatua unit are similar; containing light brown, low density clasts with a moderate vesicularity (58% Orumatua, 60% Pumice 4). The PDC deposit identified by Pardo (2012) is also similar to Pumice 4; both are poorly sorted, matrix supported, massive, and contain rounded, predominantly lapilli clasts set in a fine ash matrix.

Both the geochemistry, and textural analyses of the units confirm that Pumice 4 was most likely formed during the Oruamatua eruptive sequence. This is also supported stratigraphically where the PDC unit was found beneath 6m of other fall units, likely the Okupata eruptive units (11.6 ka) (Conway et al. 2016).

If this interpretation is correct, then this deposit provides an indication for the ‘worst case’ eruption scenario for Mt Ruapehu as the Oruamatua is the largest explosive eruption known to have occurred there (Pardo 2012).

### *Pumice 5*

The deposit was found in the valley of a small tributary to the Ohinepango Stream on the north-eastern side of Mt Ruapehu. Approximately 2 m of PDC was exposed with a lapilli fall dividing it into two separate flows. Geochemically, this unit corresponds with both the Shawcroft, and Oruamatua eruptive sequences (Figure 19) (Pardo 2012). These flows also plot within the ranges of “Unit 1” and

"Unit 2" identified by Cowlyn (2016) (Figure 17). Those two units were emplaced during the Oruamatua, suggesting that Pumice 5 was also emplaced during that time. Texturally, this deposit is similar to "Unit 1", with sub-round, whitish-grey clasts. Both deposits are also thick and found underneath other fall units. Pumice 5 is only 2 m, while "Unit 1" is approximately 6 m, though this may be due to different locations of measurement. Cowlyn (2016) identified another PDC above "Unit 1" ("Unit 2"), though this wasn't noted at the Pumice 5 locality. This also may be the result of spatial variations in the flows. While Pumice 5 was not found in a valley associated with "Unit 1", it is located in an adjacent valley, within 600m of the inferred flow path. The flows appear to have been emplaced prior to the formation of the modern ridges, which may have allowed the "Unit 1" PDC to spread further, inundating the area of Pumice 5.

This interpretation suggests that Pumice 5 was deposited during the Oruamatua eruptive sequence, between 13.6 and 11.6 ka, though prior to the emplacement of Pumice 3.

### *Pumice 6*

Pumice 6 was found on the eastern side of Mt Ruapehu and consisted of a series of ~1 m thick, well indurated outcrops draping the surface (Figure 22A). The outcrops are composed of orange pumiceous lapilli with black bombs. Geochemically, this unit corresponds with "Unit 2" and "Unit 8" (Cowlyn 2016) and the Te Herenga and Wahianoa Formations (Figure 18) (Conway et al. 2016). Neither "Unit 2" nor "Unit 8" are similar to Pumice 6, texturally. In addition to this, the deposit is found underneath a lava flow that has been mapped as the Wahianoa Formation (160-115 ka), suggesting that it was deposited prior to or during the Wahianoa Formation (Conway et al. 2016; Townsend et al. 2017). Due to the absence of any remaining evidence of the Te Herenga Formation in this area, it is likely that Pumice 6 formed between 160-115 ka in the Wahianoa Formation.

### *Pumice 7*

Found on the lower north-eastern slopes of Mt Ruapehu, this deposit is 5 m thick and located underneath approximately 50 m of lava flows (Figure 22B). Within this outcrop, there appears to be two separate flows (Figure 9E). For the purposes of this report, despite the differences in colour and geochemistry, they will be identified as the same unit with a large geochemical range. Both samples are most similar in geochemistry to the Te Herenga Formation (Figure 18) (Conway et al. 2016).

The overlying lava flows have been identified as being from the Wahianoa Formation (Townsend et al. 2017). This also suggests that Pumice 7 was deposited during the Te Herenga Formation (250-180 ka), confirming the geochemical results (Conway et al. 2016).

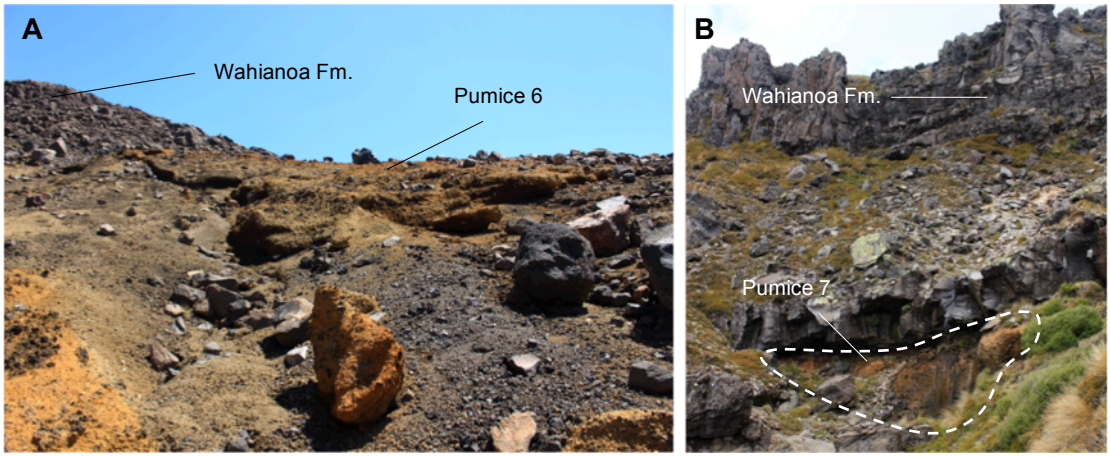


**Figure 22. Outcrop photos showing stratigraphic relationships, A) Pumice 6 deposited underneath Wahianoa lava flows. B) Pumice 7 with extensive lava flows from the Wahianoa Formation overlying it.**

### *4.1.2 Variably welded, dense PDC*

### *Dense 1*

This deposit was identified on the northern rim of Mt Ruapehu, known as Tukino Peak. This well indurated, black and red spatter deposit mantles the topography

and is relatively thick (~5 m) (Figure 23A). This outcrop overlays the Iwikau Member, constraining the timing to <10 ka (Conway et al. 2016).

Another texturally and geochemically similar outcrop to Dense 1 is located on Dome Ridge, just north of the Crater Lake. However this outcrop mantles both sides of the ridge evenly, and has no large-scale evidence of flow. Therefore, it may be an uncollapsed spatter deposit. This outcrop has been associated with the Crater Lake Member, which suggests, due to the geochemical and textural similarities, Dense 1 also occurred during the same eruptive period. This constrains the timing of Dense 1 to <4.6 ka.

### *Dense 2*

Dense 2 is located on the northern rim of Mt Ruapehu northern crater. The well indurated spatter-flow deposit is approximately 5 m thick and mantles the topography. Geochemically, Dense 2 is an anomaly in that it does not fall within the geochemistry of any previously identified unit (Figure 16). It contains a significantly lower $Na_2O+K_2O$ and CaO wt%. The most similar geochemistry is with the Mangawhero Formation (Figure 17), however this contradicts the stratigraphy. No eruptive formation can be correlated with this deposit; therefore, geochemistry is unable to be used to assist with estimating when this PDC formed.

Stratigraphically, this unit is located above the Tawhainui lava flows (6.0 ± 2.4 ka). This constrains the formation of Dense 2 to <8.4 ka. The absence of units overlying this PDC deposit makes it difficult to constrain the timing further.

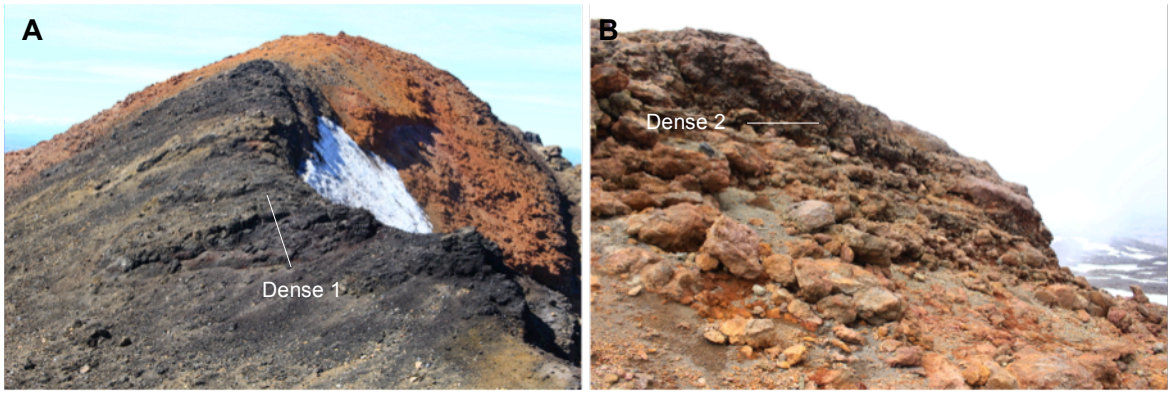


**Figure 23. Outcrop photos of Dense 1 and Dense 2. A) Dense 1 overlying older deposits from the Iwikau Formation. B) Dense 2 overlying Tawhainui lava flows.**

### *Dense 3*

Dense 3 was found on the lower northern slopes of the mountain as a variably welded, 1.5 m thick, surface deposit. Stratigraphically, it is difficult to confine the age as it is unconformably overlying the Te Herenga Formation, the oldest formation on Mt Ruapehu. The geochemistry of this unit is similar to the Whakapapa, Mangawhero, and Waihohonu Formations (Figure 18), which are all consistent with the stratigraphy.

Mapped nearby to Dense 3 is the Pinnacle Ridge Tuff unit (~10 ka), a variably welded deposit resembling a lava flow on the slopes of Pinnacle Ridge. This unit is believed to have been erupted from a nearby dike rather than the active vent (Hackett 1985). Texturally, this unit is similar to Dense 3. The Pinnacle Ridge Tuff is also described as having low CaO and MgO, consistent with Dense 3 (Figure 16) (Conway et al. 2016; Cowlyn 2016). This suggests that Dense 3 is part of the Pinnacle Ridge Tuff unit, or was deposited at a similar time, constraining the formation to ~10 ka.

While Hackett (1985) argues that the Pinnacle Ridge Tuff unit is a welded tuff rather than an ignimbrite, the apparent irregular banding similar to Dense 4 (Figure 24B) implies that the material comprising Dense 3 flowed, possibly

travelling downslope, away from the original Pinnacle Ridge Tuff unit, therefore defining Dense 3 as a “flow”.

### *Dense 4*

Dense 4 is located on the southern side of Mt Ruapehu as a large, 8 m thick, welded deposit that spans over 2 km in width intermittently. There are several outcrops of this deposit, with marginally different textures though similar compositions and stratigraphic locations. Across the entire deposit, this unit appears both above and below lava flows that form the Rangataua Member (15-10 ka) of the Whakapapa Formation (Conway et al. 2016; Townsend et al. 2017).

While geochemically the samples most resemble the compositional range of the Ngahuinga Member (48-35 ka) of the Mangawhero Formation (Figure 18), this is not consistent with the stratigraphic location. The geochemical range of Dense 4 also corresponds with that of the Whakpapa Formation, especially the Paretetaitonga (~15 ka), Rangataua (15-10 ka), and Turoa (17-10 ka) Members, which were all deposited within the same approximate time period (Conway et al. 2016). This supports the stratigraphic location of Dense 4 within the Rangataua Member, confining the age of this PDC to 15-10 ka.

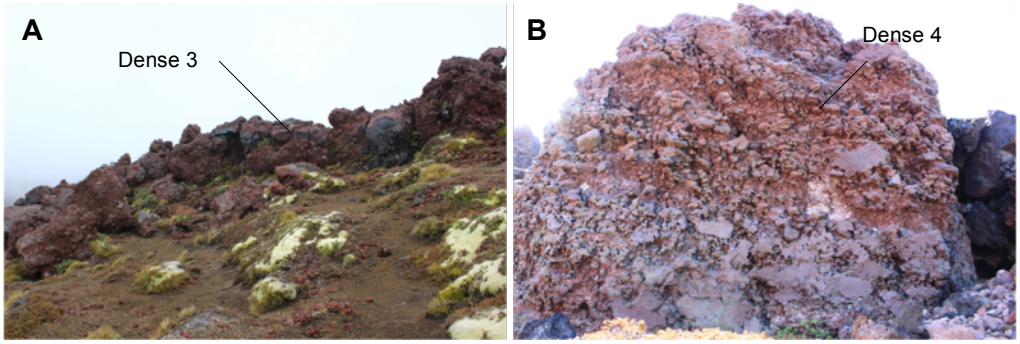


**Figure 24. Outcrop photos of Dense 3 and Dense 4. A) Dense 3 unconformably overlying the Te Herenga Formation, located under loose volcanic material. B) Dense 4, over entire outcrop appears within the Rangataua Member.**

### *Dense 5*

This PDC was found as several deposits following a small valley adjacent to the Turoa ski field on the southwestern flanks of the volcano. This well indurated, 1-4 m thick, pink and grey deposit is situated below approximately 10 m of lava flows in some locations along its length. Geochemically, Dense 5 corresponds most accurately with the Whakapapa Formation, especially the Iwikau (<10 ka) and Turoa (17-10 ka) eruptive packages (Figure 18). Stratigraphically, this unit is located within Turoa Member lava flows, confirming that it was deposited at the same time. This constrains the timing of PDC deposition to between 17-10 ka.

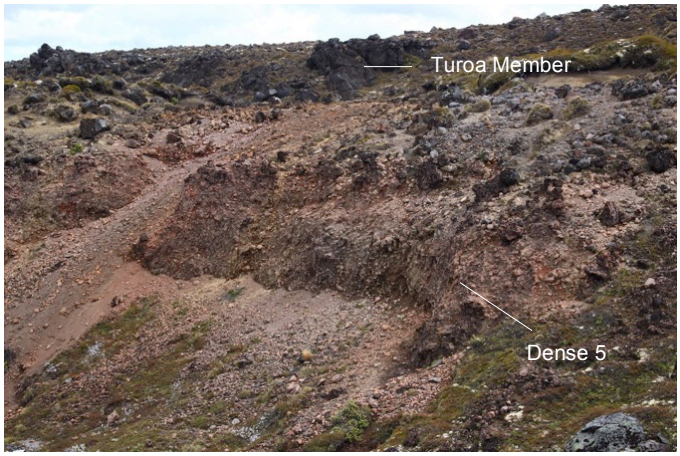


**Figure 25. Outcrop photo of Dense 5 with overlying Turoa Member lava flows.**

## *4.1.3 Scoria-dominated, small volume PDC*

### *Scoria 1*

This small volume scoriaceous deposit outcropped on the western side of Mt Ruapehu next to the Mangaturuturu Glacier (Figure 26B). The unit has been deposited above a lava flow part of the Turoa Member of the Whakapapa Formation, constraining the age of the PDC to <11.7 ka (Townsend et al. 2017). Geochemically, this unit also plots within the range of the Whakapapa Formation (Figure 18). In the field it can be seen that the Turoa Member lava flows had

undergone significant erosion prior to the deposition of Scoria 1. This suggests that Scoria 1 is more recent than 11.7 ka. Nearby this unit there are mapped deposits part of the Crater Lake Member. Though Scoria 1 does not geochemically correlate with the single sample obtained by Conway et al. (2016) (Figure 18), it is possible that with more samples, the range of compositions would correspond. This conclusion is supported by Townsend et al. (2017) who also noted the presence of a PDC in this area, though did not elaborate.

Overall, Scoria 1 provides evidence for relatively recent activity from the Crater Lake vent, forming PDCs. Flows in this formation have been dated at 0.2 ± 2.2, and <4.6 ka (Conway et al. 2016), thus constraining the occurrence of Scoria 1 to <4.6 ka.

### *Scoria 2*

Scoria 2 was found below the Mangatoetoenui Glacier as a 4 m thick, well indurated, black outcrop (Figure 26A). Due to the amount of debris in this area, it is difficult to determine whether Scoria 2 is underlying the adjacent lava flows or was deposited more recently. Based on the apparent dip on the outcrop and its unconformable behaviour compared with the topography, it is assumed that the PDC was deposited prior to the lava flows.

Geochemically, the deposit is comparable to the Whakapapa, Mangawhero, and Wahianoa Formations (Figure 18). The overlying lava flows are the Tawhainui flows (6.0 ± 2.4 ka) (Townsend et al. 2017). It appears that Scoria 2 occurred subsequent to the Mangatoetoenui lava flows (9.2 ± 8.0 ka) (Conway et al. 2016). This constrains the deposition of this unit to the Whakapapa Formation, between 9.2 ± 8.0 and 6.0 ± 2.4 ka, though prior to Pumice 1, based on the stratigraphic relations.

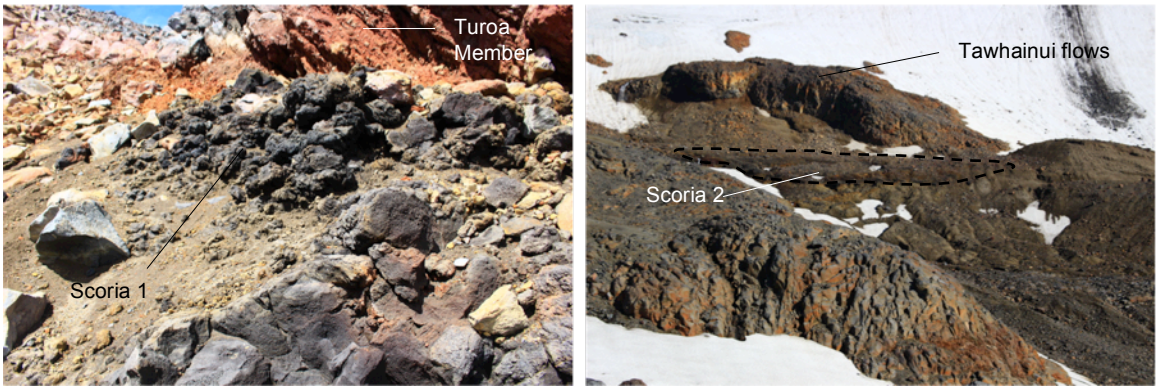


**Figure 26. Outcrop photos showing stratigraphic relationships, A) Scoria 1 located above heavily eroded Turoa Member lava flows. B) Scoria 2 outcropping below Tawhainui flows and above the Mangatoetoenui lava flows.**

### *4.1.4 PDC timeline*

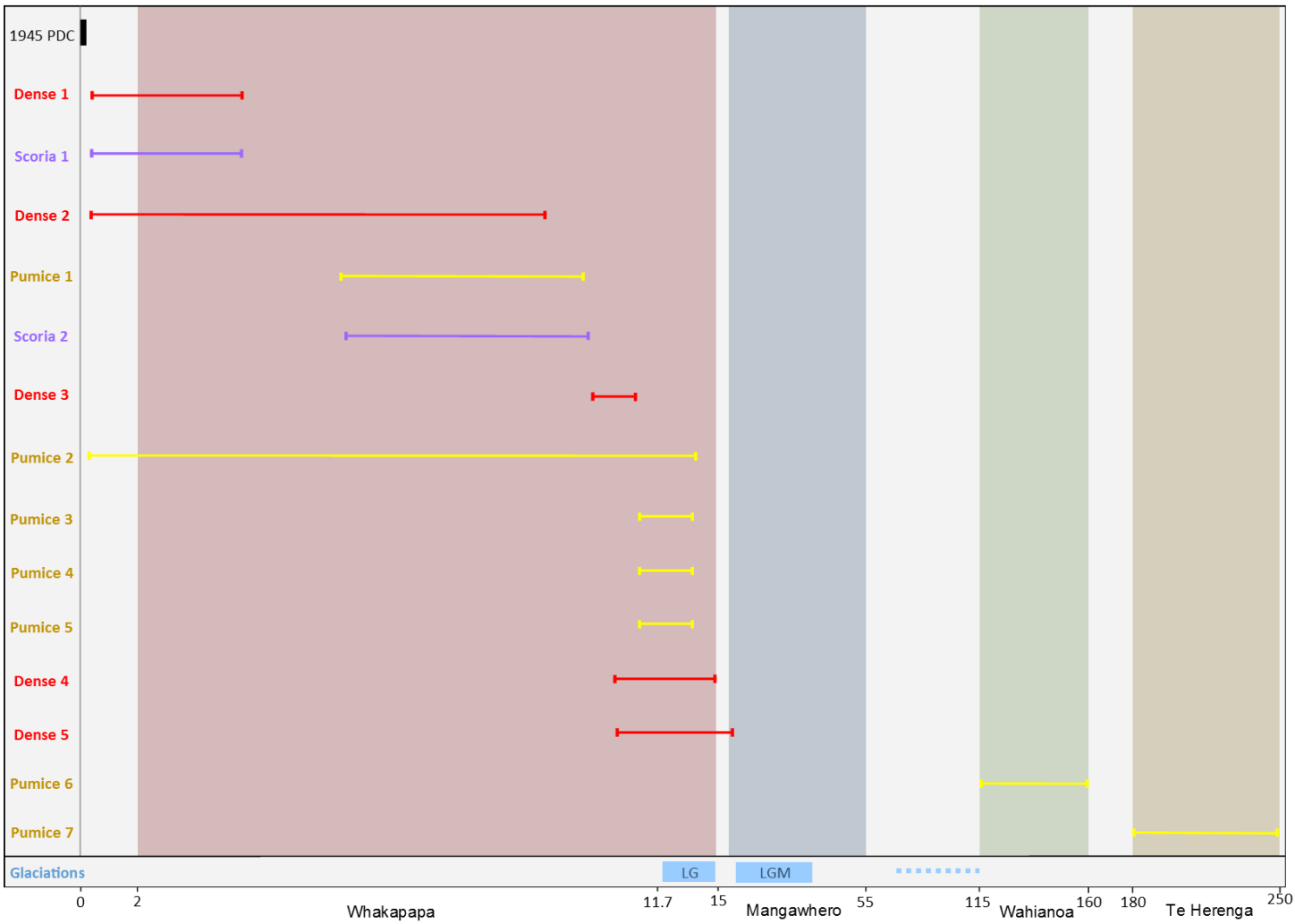


**Figure 27. Possible age ranges of PDCs identified during this study and the known 1945 PDC. Coloured blocks are formations identified by Conway et al. (2016), and the glaciations at Mt Ruapehu are represented by the blue bars (LG is the last glacial, LGM is the last glacial maximum). The dotted blue line indicates fluctuating glacial extents (Eaves 2015). Age axis is not to scale.**

Figure 27 shows the temporal distribution of PDCs identified in the study as well as the 1945 PDC. Pumice 6 and Pumice 7 are the oldest deposits, occurring prior to a glacial period. They were likely preserved by signficant lava flows burying them before advancing glaciers eroded the deposits. There is an apparent absence of PDCs during the glacial period, and after the last glacial at Mt Ruapehu the occurrence of PDCs increases significantly. These distributions will be discussed further in Section 4.3.

## 4.2 Eruption style

PDCs can be formed by a variety of different eruption styles such as collapsing Plinian/sub-plinian eruption columns, collapsing Vulcanian eruption columns, gravitational failure of a lava dome, collapsing agglutinated pyroclastic material or the toe of a lava flow (Nairn & Self 1978; Rodríguez-Elizarrarás et al. 1991; Stinton & Sheridan 2008; Buchwaldt 2013). It is assumed that the textural characteristics of the PDC deposits will reflect their formation mechanism (Barker et al. 2012; Brown & Andrews 2015). Characteristics such as vesicularity, grain size, and flow size will be used to infer an approximate eruption style and intensity. The intensity and magnitude of the eruption will be measured using the volcanic explosivity index (VEI) (Newhall & Self 1982). PDC deposits from international case studies are used to support these results. It is important to note that this is based on rapid fieldwork on a whole volcano scale and only limited sampling possibilities. Many factors influence eruption style, which are difficult to assess quickly in the field and within the scope of an MSc, such as magma viscosity, and, although I consider the bulk geochemistry, it is also necessary to consider other factors that influence viscosity, such as temperature and volatile content (Bottinga & Weill 1972; Baker & Alletti 2012; Kilgour et al. 2016)

### *4.2.1 Pumiceous PDC*

The grain size distribution of these deposits confirms that these are PDC deposits rather than airfall deposits, consistent with the field PDC confidence

ranking of moderate confidence. The broader range of grain sizes in PDCs compared with airfall corresponds with the distributions identified by Walker (1971) (Figure 28). The significant proportion of fine grain sizes compared with airfall also suggests that some degree of mechanical abrasion has occurred, which is indicative of the processes forming a PDC (Branney & Kokelaar 2002; Buckland et al. 2018).

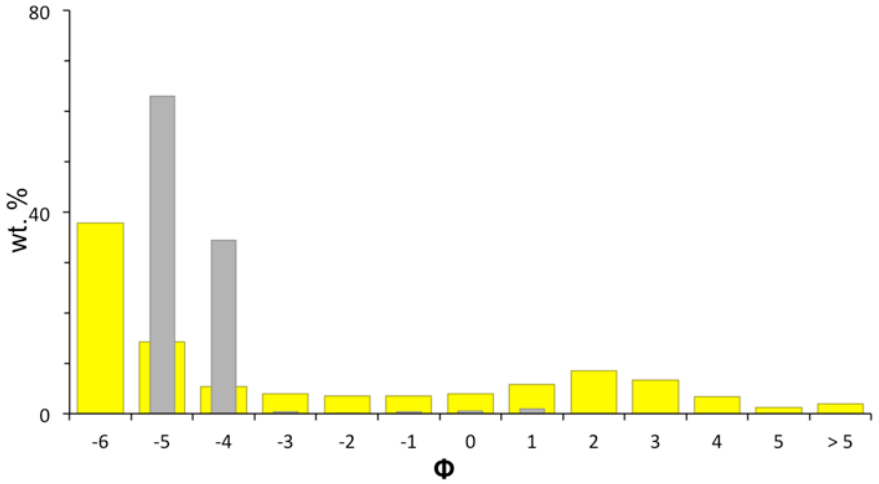


**Figure 28. Grain size distribution of standard pumiceous PDC deposit (yellow) compared with a Ruapehu airfall sample (grey). Airfall data displays a different distribution than the PDC deposits, with a single peak and narrow grain size range.**

This flow type is characterised by a low density (0.83-0.31 g/cm$^3$), high vesicularity (50-60%), and a large flow distance (>3 km). The low density and high vesicularity of the clasts within the flows are indicative of an explosive eruption, where the gases exsolved quickly during a rapid magma ascent (Pardo 2012). The distance this type of PDC travelled indicates that a lot of material was produced during the eruption, suggesting it was a large eruption, such as a Plinian or sub-plinian. This is consistent with implications of Pardo et al. (2012a) and the observations and classifications of Cowlyn (2016).

PDCs generated by Plinian and sub-plinian eruptions produce extensive pumice and ash-rich deposits, up to 20,000 km$^2$ (Brown & Andrews 2015). The

PDCs in this group were calculated with minimum areas ranging between 0.03-4.2 $km^2$. This value is significantly lower than other Plinian to sub-plinian PDCs, likely as these are only conservative flow path estimates, and much of the deposit may have been eroded over time. Most of these calculated values are marginally lower than those identified by Cowlyn (2016), 0.90-2.66 $km^2$. The lesser values can also be potentially explained by more conservative flow path estimates or the occurrence of smaller flows. More outcrops were identified in this study as being part of the largest flow identified by Cowlyn (2016) (2.66 $km^2$), thus extending the approximate area to 4.2 $km^2$. The interpreted runout distances were between 3-9 km. The well-rounded clasts in these deposits also suggest a significant travel distance, as well as a large, energetic flow (Kueppers et al. 2012).

An analogous PDC deposit from a historic eruption is the 1991 Pinatubo (Philippines) eruption, where a large Plinian eruption column collapsed to create PDCs that travelled at least 8 km away from the vent (Rosi et al. 2001). The PDC deposits were massive, pumiceous and poorly sorted, and contained a range of grain sizes. These characteristics are comparable to pumiceous PDC deposits found on Mt Ruapehu, indicating that a collapsing Plinian or sub-plinian eruption column (VEI 3-5) may have produced these deposits (Figure 29).

This hypothesis is also supported by the known occurrence of Plinian and sub-plinian eruptions on Mt Ruapehu (Pardo 2012). Within these Plinian tephra deposits Pardo (2012) identified thin, poorly sorted layers hypothesised as PDC deposits from unsteady, collapsing columns.

This style of PDC was also identified by Cowlyn (2016) who also noted a bimodal grain size distribution in some deposits with bomb-sized clasts in an ash matrix. Geochemically, the both groups display a similar $SiO_2$ range, though the pumiceous PDCs identified in this study display a greater range in MgO and CaO compositions (Figure 16). Texturally both groups are similar, exhibiting poorly

sorted and primarily matrix supported outcrops containing sub-rounded pumice clasts with a varying degree of lithics in each unit (Cowlyn 2016). As noted previously, the flow extents are also similar in length with a comparable estimated flow area.

The high vesicularity and relatively low proportion of very fine grain sizes (>4$\Phi$) suggests that the eruptions that formed these PDCs were magmatic rather than phreatomagmatic. This is inferred as external water causes magma to quench immediately and undergo a greater degree of fragmentation, resulting in finer grain sizes (Brown & Andrews 2015). The vesicles in magmatic clasts continue to expand even after being erupted, resulting in a higher vesicularity (Hiroi & Miyamoto 2016).

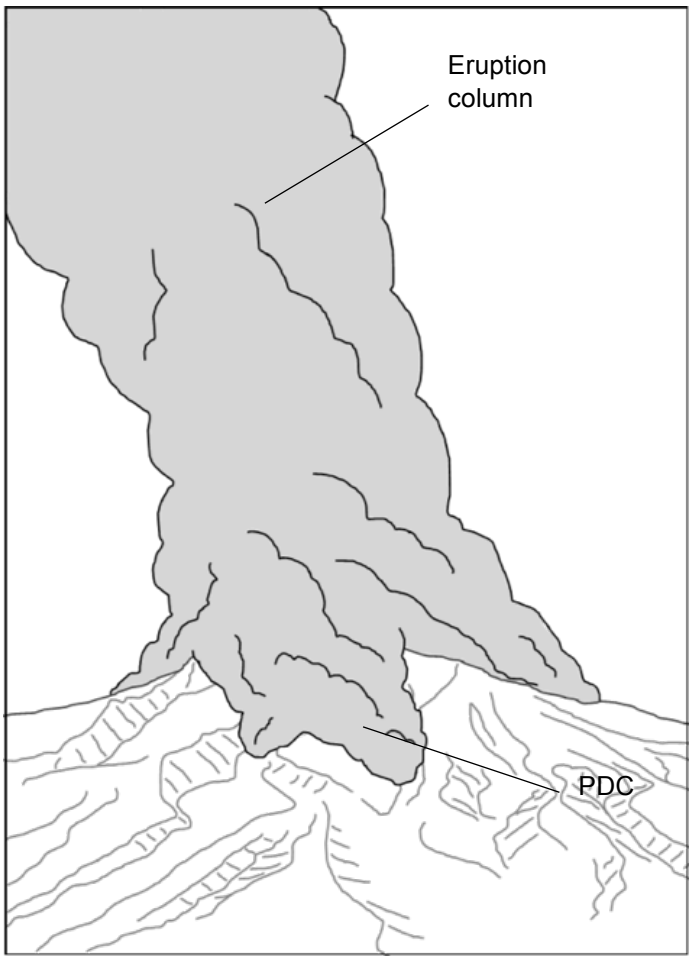


**Figure 29. Collapsing Plinian/sub-plinian eruption column forming a PDC, corresponding to the pumiceous PDC group identified in this thesis.**

### *4.1.2 Variably welded, dense PDC*

As noted in the results, these deposits were identified with "very high confidence" as PDCs, lava breccia, and spatter deposits. The absence of lava units above or below some of the units was used to eliminate the possibility of lava breccia in some instances. While spatter components were identified in some outcrops, reinforcing the possibility of a spatter deposit, these spatter layers were confined to small areas of the flow. Minor reverse grading and broken clasts were used as evidence that these deposits have travelled down slope, suggesting that they are PDCs. This is also supported by the occurrence of a fine-grained ash matrix surrounding the clasts and the presence of lithics within the flow. These features indicate the material flowed down slope, generating an ash matrix and incorporating lithics from the substrate. The presence of spatter textures will be discussed later in this section.

These deposits are characterised by sub-rounded, relatively denser (1.31-1.58 g/cm$^3$), and less vesicular clasts (1-30%), as well as a variable degree of welding. The red colouration and fluidal textures of clasts seen in some deposits indicate that these flows were deposited while still ductile and hot, and have undergone thermal alteration (Walker & Croasdale 1971; Cowlyn 2016). The moderate to high densities and low vesicularity in these deposits indicates that the eruptions were either less explosive or underwent some degree of vesicle collapse or compaction. The possibility of vesicle collapse and compaction is supported by the ductile nature of some clasts. This fluidity and welding of the clasts is similar to those seen in spatter deposits during Strombolian or Hawaiian fire-fountaining eruptions (Houghton & Gonnermann 2008). However, given that these deposits were found a significant distance from the vent suggests either this was a spatter-fed PDC, or that the accumulated spatter deposit underwent gravitational collapse and travelled downslope, forming a PDC (Mellors & Sparks 1991). The size and volume of the deposits indicates that the PDCs were being constantly fed with material, such as during a sustained Strombolian eruption, rather than a single collapse event.

The PDCs in this group were calculated with minimum areas between 0.03-2.47 $km^2$, similar to those calculated by Cowlyn (2016) (0.90 $km^2$). The greater range in values in this study is due to a greater amount of deposits being found. The interpreted volumes in these deposits range between 18-990 $x10^{-5}$ $km^3$, which have a larger range, though are similar to those calculated by Cowlyn (2016) (100-600 $x10^{-5}$ $km^3$). The runout distances in this group were between 1-5 km, lower than the pumiceous PDC group, likely due to a lower eruption volume and less energetic emplacement. This results in a flow with less momentum, preventing it from travelling significant distances and spreading out. This forms a thicker deposit, with a higher aspect ratio (Table 1), which is also seen in the scoria-dominated PDC group.

This type of deposit is also seen in Santorini (Greece) and during the Onano eruption, Vulsini Volcanoes (Italy). In Santorini, spatter-rich flow deposits were found nearly 8 km from the inferred vent (Mellors & Sparks 1991). These deposits are similar to those found at Mt Ruapehu in that they both display moderate to poor vesicularity and are found far from the vent. The Santorini deposits have densities between 1.7-1.9 $g/cm^3$. These denser clasts at Santorini are likely caused by greater vesicle collapse and compaction or potentially an initially lower gas content and lower explosivity. The vesicle morphology is also unique to this group. Where other eruption styles demonstrate sub-spherical bubble, the vesicles in this group are usually irregular and rough (Figure 13), which may be the result of deformation and compaction upon collapse of the spatter while it was still hot. Overall, the textures seen in this flow group are comparable to other spatter flows described in literature (Mellors & Sparks 1991; Valentine et al. 2000; Carracedo Sánchez et al. 2012).

Based on these characteristics and the similarities in other analogous deposits, it is likely that the variably welded, dense PDCs were formed during a

sustained Strombolian style eruption (VEI 1-2), where the PDCs were being constantly fed by spatter while they flowed downslope (Figure 30).

This deposit type and eruption style was also identified by Cowlyn (2016). Both studies found variably welded, matrix supported deposits with sub-rounded, vesicular clasts showing evidence for hot emplacement. Though, the vesicularities identified here are lower than what was identified by Cowlyn (2016) (~60%). Geochemically, the deposits in this study have a greater range in $SiO_2$ and are generally lower in MgO.

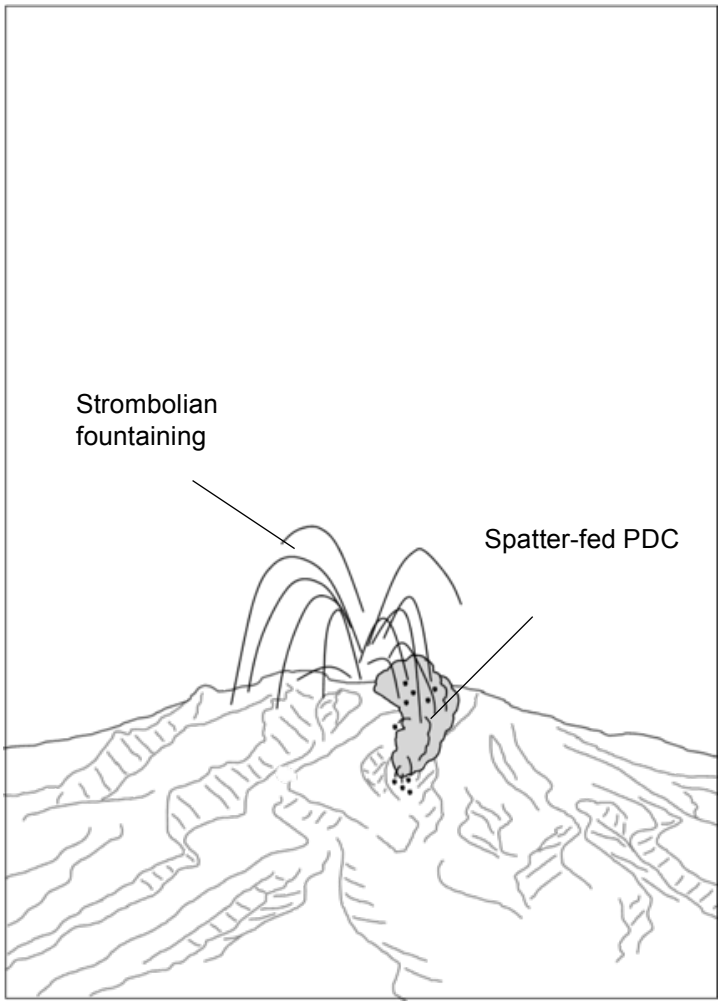


**Figure 30. PDC forming from collapsing Strombolian spatter, correpsonding to the variably welded, dense PDC in this thesis. The erupted spatter continues to sustain the flow as it travels downslope.**

### *4.1.3 Scoria-dominated, small volume PDC*

This deposit type is distinguished by its small volume and extent (0.9-1.3 km), moderate density (1.14-1.41 g/cm$^3$) and moderate vesicularity (40-45%), and black scoriaceous clasts. The large density distribution (Figure 12) overlapping with other eruption styles is likely explained by variations in eruption intensity, or by the expansion of vesicles after eruption (Hiroi & Miyamoto 2016). The low density and moderate vesicularity of the deposits suggest they formed during a small explosive eruption. The small volume of these flows also confirms this, as they were likely generated during a short-lived, small eruption where little material was produced. Example of small volume, explosive eruptions include Strombolian, sub-plinian or Vulcanian. Deposits from Strombolian eruptions have already been noted during this study, where the density was greater (1.31-1.58 g/cm$^3$), and contained small, deformed vesicles (1-30%). As inferred sub-plinian eruptions have also been identified, sometimes several kilometres from the vent, it is likely this deposit type was formed during small, explosive, and short-lived Vulcanian eruptions.

The PDCs in this group had interpreted minimum areas of 0.028-0.066 km$^2$, lower than what was calculated by Cowlyn (2016) (0.15-0.17 km$^2$), though this may be due to more conservative estimates, or smaller eruptions. These PDC deposits were also found within 2 km of the vent, whereas Cowlyn (2016) identified deposits over 4 km away. The calculated volumes ranged between 3-13 x10$^{-5}$ km$^3$, which overlaps with the values from Cowlyn (2016) (3.9-200 x10$^{-5}$ km$^3$), though is generally lower.

Similar textural characteristics to this group were also noted during other Vulcanian eruptions, such as the 1975 Ngauruhoe sub-plinian to Vulcanian eruption, which generated PDCs through a small column collapse. These clast densities ranged between 1.1-1.3 g/cm$^3$ (Nairn & Self 1978), which are similar values to those calculated during this study. The 2013/14 Vulcanian eruptions at Tungurahua volcano in Ecuador also present similar textures with well-rounded,

vesicular andesite clasts with spherical bubbles and densities between 1.5-1.6 g/cm$^3$ (Hall et al. 2015).

Based on the textural characteristics and similarities to other eruptions, it is likely that the scoria-dominated, small volume PDC group was generated during small, short, explosive Vulcanian eruptions (VEI 2) (Figure 31).

Cowlyn (2016) also identified this textural group and eruption style, with both groups containing black cauliflower, and breadcrust bombs. Though the clasts in this group did not contain any orange banded clasts as was identified by Cowlyn (2016). Geochemically, the deposits identified by Cowlyn contain a greater range in $SiO_2$, though the deposits in this study are similar (Figure 17). The deposits in this group fall within the MgO/CaO range identified by Cowlyn (2016) (Figure 16).

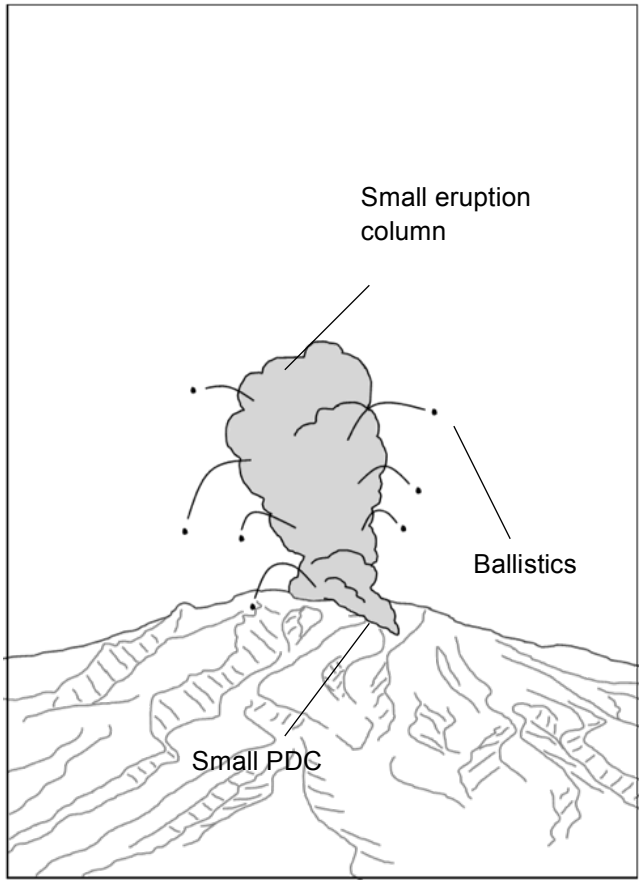


Figure 31. A short, explosive Vulcanian eruption forming a scoria-dominated, small volume PDC

### 4.3 Preservation of flows

The poor preservation of volcanic material, especially unconsolidated volcaniclastic material such as PDC deposits, on glaciated volcanoes is a significant issue when identifying past events and when determining the probability of future events. When deposited on snow or ice, pyroclastic material can trigger syn-eruptive floods or lahars (e.g. Nevado del Ruiz) (Thouret et al. 2007). In addition to being a hazard to nearby infrastructure and people, this also remobilises the material and erases the original flow deposit. The pyroclastic deposit is also removed from the record upon seasonal or gradual melting of the snow or ice (Manville et al. 2000).

Volcanic material deposited onto rock can also be removed by glacial advance and erosion. As a glacier flows downslope, it plucks and abrades the underlying substrate (Knight 1999). Through this process, unconsolidated PDCs, are likely to be fully eroded during glacial advances and redeposited as glacial moraines (Eaves et al. 2016; Townsend et al. 2017).

Mt Ruapehu is a glaciated volcano that had extensive ice cover during ~35-18 ka with a minor glacial advance between ~15-11.5 ka (Figure 32) (Eaves 2015; Conway et al. 2016). This suggests that PDCs that occurred during these times are unlikely to have been preserved in the geological record. To be preserved, a PDC would have had to flow past the ice margin and out of drainage channels. This poor preservation is evident in Figure 27, where there is an absence of PDC deposits prior to 15 ka. After 15 ka, the occurrence of PDCs in the geological record increases significantly. This coincides with the glaciation dates for Mt Ruapehu—once the glaciers retreated, the preservation potential for PDCs improved.

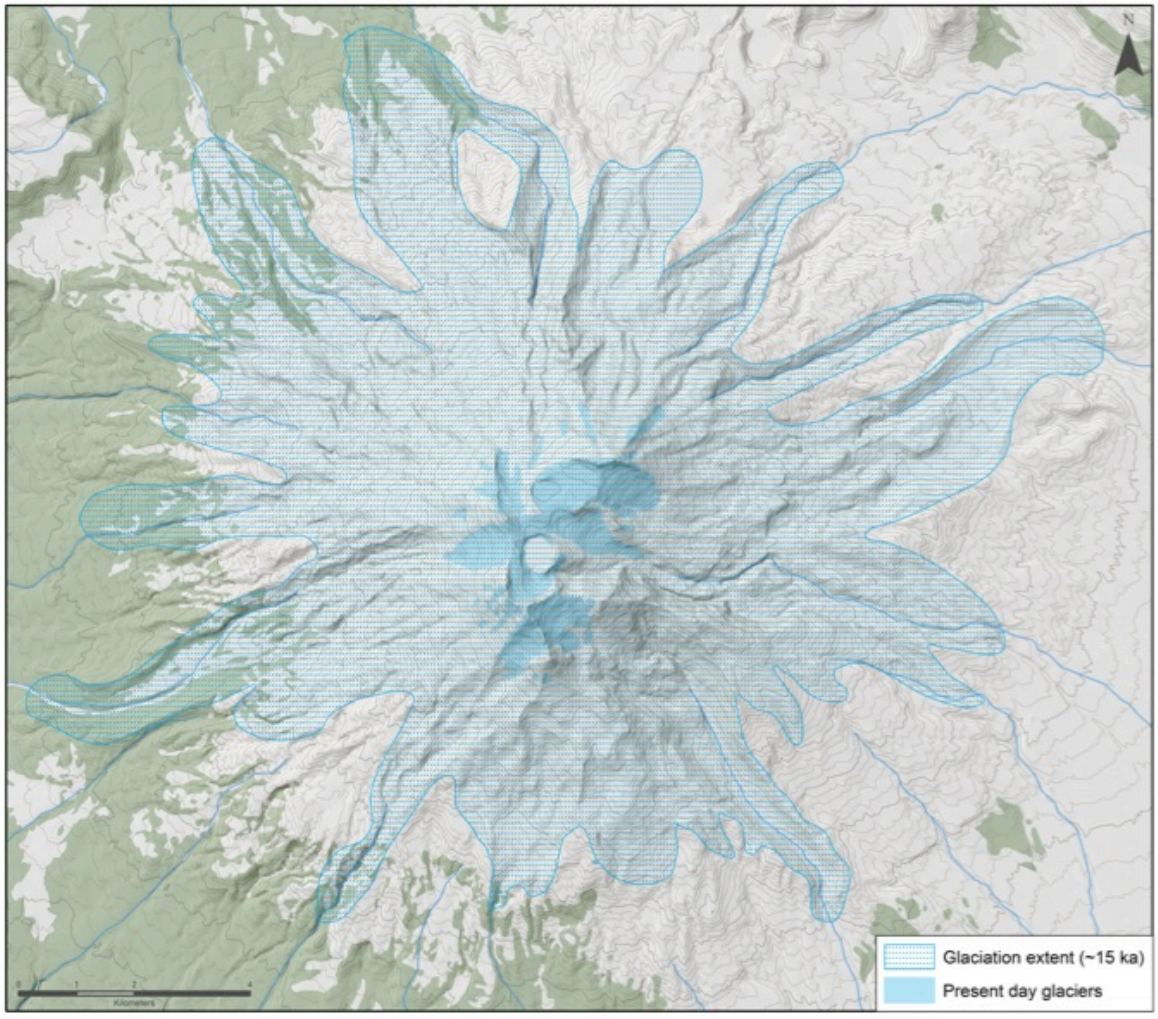


**Figure 32. Glacial extent of last glacial maximum at Mt Ruapehu. Adapted from Eaves et al. (2016). PDCs occurring during this time are unlikely to have been preserved if deposited on the ice. As the snow and ice melts the PDC deposits would be removed and remobilised in river valleys. PDCs may have been preserved if they flowed past the maximum ice extent.**

During interglacials, such as present day, the preservation of PDCs may still be hindered by the presence of snow. Snow covers most of the volcano during winter. The deposition of PDCs or tephra onto snow can lead increased melting from a lower albedo, syn-eruptive lahars, sheetwash, ash-induced avalanches, or slumping from overloading (Manville et al. 2000). All of these processes remobilise and remove the original deposit. There is almost no stratigraphic record of the over 40 eruptions in the past 100 years at Mt Ruapehu, proving the effectiveness of these processes at removing volcanic deposits from

the record (Manville et al. 2000). Therefore, if a small volume PDC was generated recently during winter, it is unlikely that there would be any record of its occurrence.

The preservation potential of PDCs is also affected by the extent, volume, type of flow, and how quickly they were buried by subsequent volcanic deposits. The two oldest flows identified in this study were large pumiceous PDCs that were found underneath lava flows. This suggests that the lava flows buried the PDC deposits soon after deposition, preserving them. The next oldest deposits were the thick, variably welded deposits that were likely preserved due to the volume and induration of the flows. The small volume PDCs were some of the youngest identified, and had the least deposits found. It is likely that the low volume and usually poor induration allowed the majority of these deposits to be eroded.

Another factor that may influence the preservation of PDCs is the topography and slope gradient. When the PDC first begins to flow it may not deposit any material, and instead could erode the substrate on steep slopes. The PDC begins to deposit material once it slows down or the slope gradient lessens. This is observed on volcanoes like Ngauruhoe, where there was no deposition of the PDC at angles greater than ~30° (Lube et al. 2007). This also contributes to the difficulties in identifying PDCs as they often only appear on the lower slopes, with no evidence of some flows having been deposited on the upper slopes.

One of the leading limitations of this study was the poor preservation of these deposits. In all of the PDCs found, most of the deposits had been eroded away. This hindered analyses, and estimations of thicknesses and extent of the flows. While other studies have estimated the original volume of ignimbrites while taking into account erosion (Wilson 1991), this was not feasible to do within the scope of this study. Therefore, while the flow extent was estimated based on the

current deposit thickness, the original thickness of the deposits was not considered.

Due to the number of variables affecting the erosion and preservation of these deposits (volume, induration, extent, glaciation, season), the amount of PDCs eroded away or the total occurrence of PDCs is unable to be quantified.
It is important to consider the poor preservation of the PDCs as this section indicates that the PDC hazard could be severely underestimated when using the deposits identified in this paper or by Cowlyn (2016) as there may no longer be a record of most prehistoric PDCs.

## 5. Limitations

In addition to the limitations associated with each individual method, there were other limitations that hindered the overall accuracy of this study.

The short time frame, and breadth of this study resulted in a restricted methodology, where some analyses, such as age dating, were unable to be conducted. Age estimation based on stratigraphy and geochemistry had to be utilised instead. Due to the short time frame, only locations where PDC deposits were suspected were visited, leaving much of Mt Ruapehu unexplored. Therefore, there is a possibility that some PDC deposits were not located, hindering the PDC occurrence and frequency estimation.

As previously mentioned in Section 4.3, most identified outcrops had been heavily eroded with little of the original deposit remaining. This limited the accuracy of field observations as the thickness and extent may have been altered over time. In order to determine an approximate volume and flow path the discontinuous outcrops had to be extrapolated, incorporating further uncertainty into the analyses. These small outcrops also made characterisation of the deposit difficult, as there was often not enough of the deposit exposed to see a

cross-sectional view or spatial variations within the flow. The absence of most prehistoric PDCs also limits the estimation of PDC occurrence and frequency on Mt Ruapehu.

Despite these limitations however, the aim of using rapid, simple methods for assessing the PDC hazard when mapping a large stratovolcano was achieved. This proves the usefulness of applying these methods for a large scale and short time frame project, with an understanding of the limitations involved with these techniques.

## 6. Future work

While this study is a step forward in improving the understanding of PDCs on Mt Ruapehu, further work is required to build on it and better understand the potential hazard. For example, finding the 1945 PDC deposit may help to characterise the size and type of PDCs that can occur during present day. This also includes constraining the ages of the PDCs using further mapping, age-dating where crystalline groundmasses allow, and investigating the potential future PDC flow paths using modelling. It is also important to build on the PDC frequency and identify a PDC occurrence probability for each eruption style. These are crucial components for hazard awareness and mitigation during future eruptions.

This type of study can potentially be used to inform event trees for volcanic crises at Mt Ruapehu (Newhall & Hoblitt 2002) that can be used to assess probabilities of PDC types. For example, using the last 160 years of eruption data at Mt Ruapehu and combining it with the only known PDC during this time (1945), a rudimentary event tree can be created (Figure 33). However, this event tree underestimates the occurrence of PDCs during other eruption styles, when this study has shown that they have occurred over a longer timescale. Therefore, it is important to incorporate PDCs from the geological record into future event trees and hazard analyses. However, more data is

needed to make a meaningful attempt at a PDC event tree incorporating the whole history of the volcano. Although this study makes a significant step towards reducing the error on number and timing of different PDCs at Ruapehu, I encourage rigorous uncertainty analysis to make these numbers useful to hazard modellers.

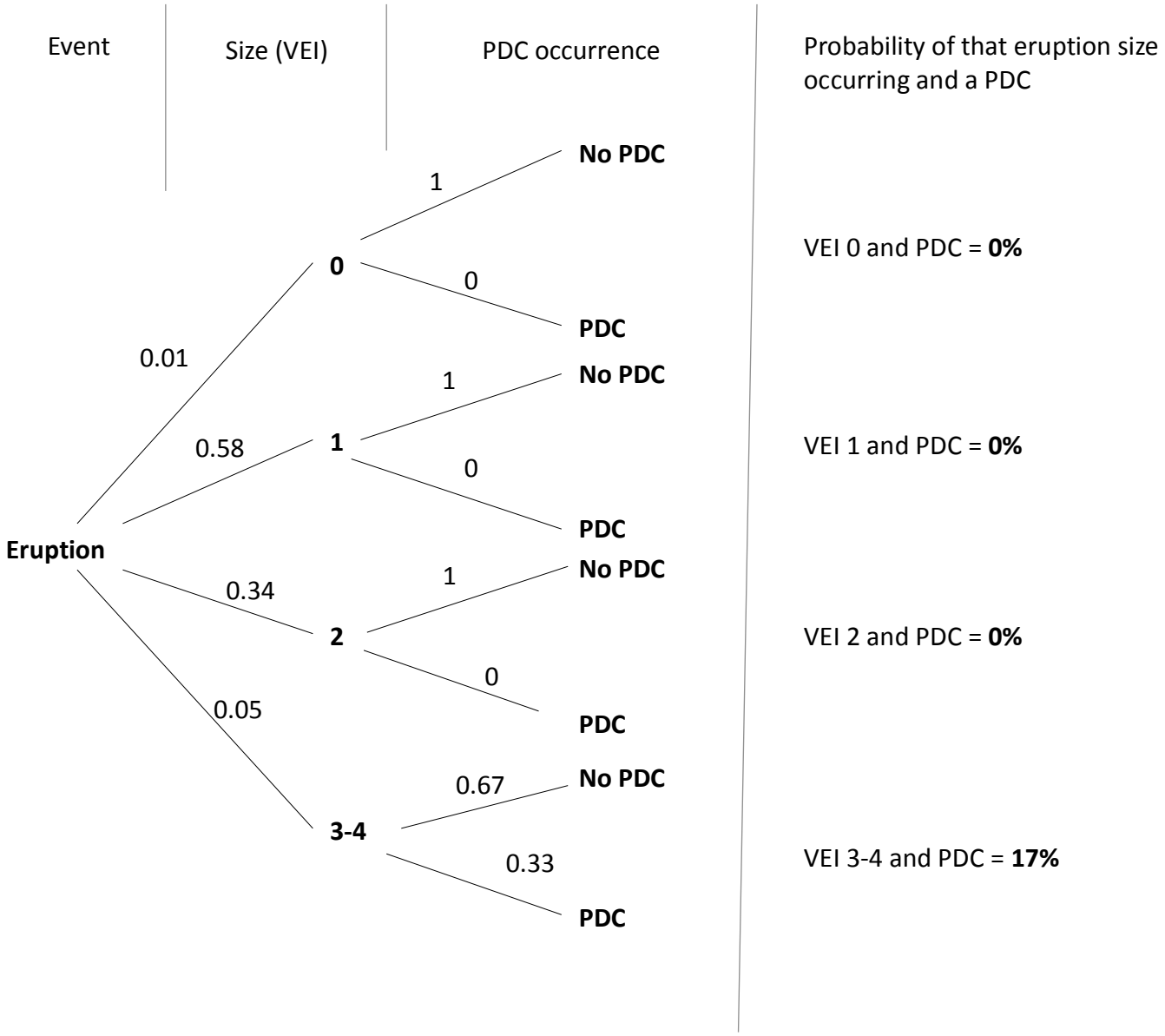


**Figure 33. Example event tree created using eruptions from the last 160 years at Mt Ruapehu, and the only known PDC to have occurred during that time (1945). This event tree underestimates the occurrence of PDCs from smaller eruptions, when this study has shown that they have occurred over a longer timescale.**

# 7. Conclusions

Pyroclastic density currents are a significant hazard due to their speed, temperature, and flow path unpredictability. This means that it is vital to understand the PDC hazard at volcanoes where people may be at risk from such a hazard. The aim of this study was to increase the awareness of the potential PDC hazard at Mt Ruapehu by confirming the occurrence of multiple PDCs in the past. PDC deposits were identified, characterised, and assigned an eruption style. This was achieved through extensive field work, a confidence-based identification chart (Cowlyn 2016), grain size distributions, density and vesicularity analyses, and whole rock major element geochemistry.

Overall, 14 PDC deposits were found. When combined with the deposits identified by Cowlyn (2016) and the known 1945 PDC, this is a total of 24 PDCs preserved throughout the history of Mt Ruapehu (Figure 34).

The PDCs recognised in this study were separated into 3 textural groups:

- Pumiceous, large volume PDC
- Variably welded, dense PDC
- Scoria-dominated, small volume PDC

The pumiceous PDC group was determined as having formed during a sub-plinian or Plinian eruption due to the clast textures and extent of the flows, and made up the greatest proportion of PDCs identified on Mt Ruapehu. The Plinian PDC-forming eruptions have been occurring since 250 ka, and have a geochemical range of 54.38-58.48 wt% $SiO_2$, and 3.58-6.5 wt% MgO. The variably-welded, dense PDC formed by the gravitational collapse of a spatter rampart or sustained fountaining created during a Strombolian, fountaining-style eruption. These PDCs are estimated as having occurred since 17 ka and have geochemical ranges of 56.18-60.16 wt % $SiO_2$, and 2.52-4.82 wt% MgO. It is likely that the scoria-dominated, small volume PDC formed from shorter lived, small volume Vulcanian eruptions, based on lesser flow extent of this group of

PDCs. These eruptions are only preserved since 9.2 ka and have a small geochemical range of 58.69-58.85 wt% $SiO_2$, and 4.25-4.58 wt% MgO.

This work extends the knowledge of PDCs on Mt Ruapehu to >180 ka. Consistent with findings of Cowlyn (2016) and Pardo (2012) there is an abundance of PDCs after 15 ka. We conclude that this is due to a combination of poor preservation of the deposits during glacial maximums on the mountain but also due to the shift to Plinian-style eruptions which produced larger PDCs more likely to be preserved. However, poor preservation, particularly of small volume PDCs, needs to be considered in the future when attempting to quantify the frequency of PDCs.

Overall, this study provided additional important evidence of the PDC hazard on Mt Ruapehu, where PDCs are possible from Strombolian, Vulcanian and Plinian eruption styles, and thus are both a near-vent (proximal) and distal hazard. This study did not reveal any strong evidence for phreatomagmatic-driven PDCs, although this needs to be considered given the currently well-established Crater Lake and the uncertainty around the PDC erupted in 1945. In summary, the evidence presented here necessitates continued comprehensive studies to gain a better understanding of future PDC occurrence, and the threat they pose to nearby infrastructure and communities.

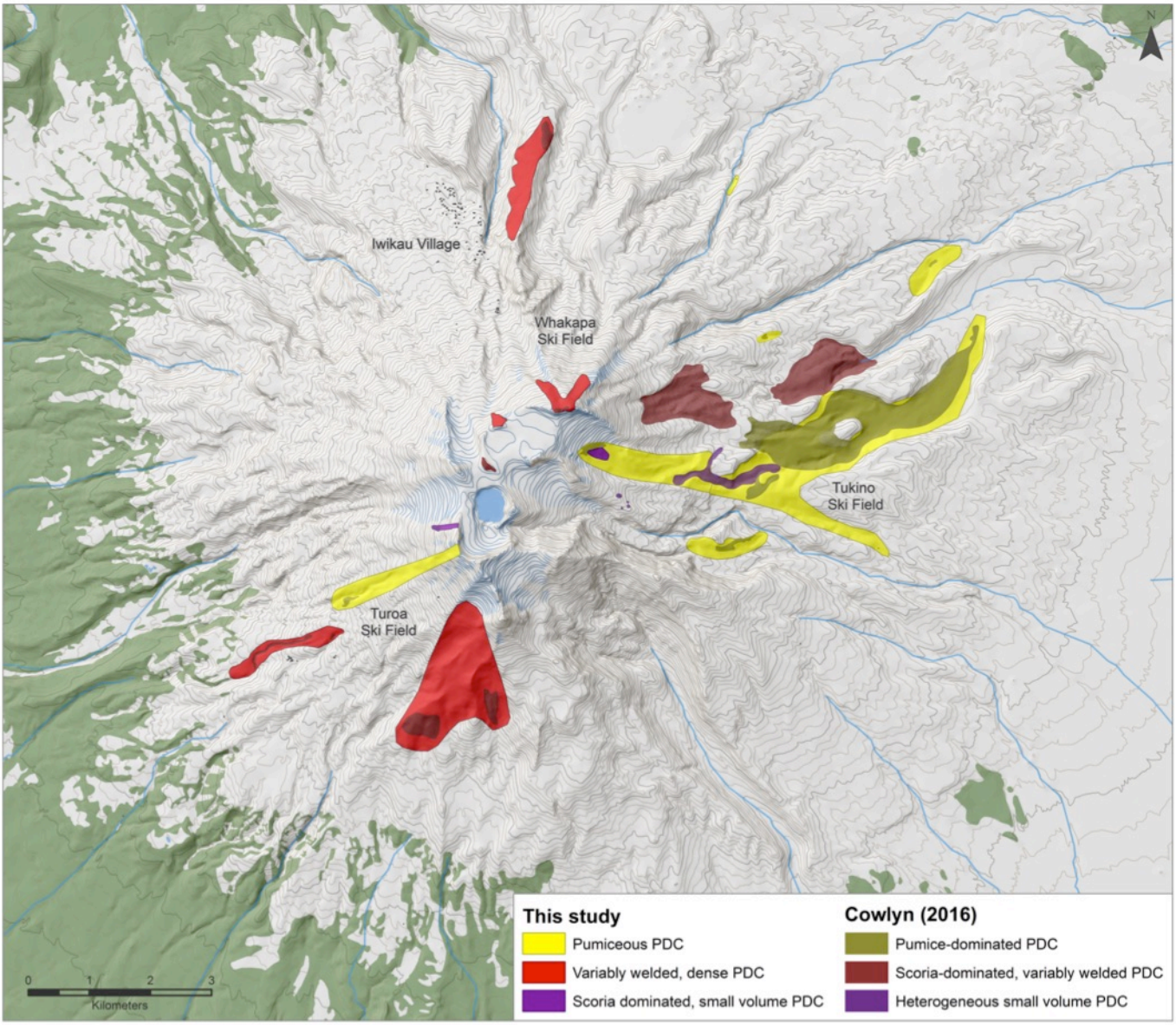


**Figure 34. Final PDC map of Mt Ruapehu, combining PDCs from this study and Cowlyn (2016). There is a total of 24 PDCs identified, including the 1945 PDC (not mapped).**

## References


Auker MR, Sparks RSJ, Siebert L, Crosweller HS, Ewert J 2013. A statistical analysis of the global historical volcanic fatalities record. Journal of Applied Volcanology 2(1): 1-24.

Baker DR, Alletti M 2012. Fluid saturation and volatile partitioning between melts and hydrous fluids in crustal magmatic systems: The contribution of experimental measurements and solubility models. Earth-Science Reviews 114(3-4): 298-324.

Barker SJ, Rotella MD, Wilson CJN, Wright IC, Wysoczanski RJ 2012. Contrasting pyroclast density spectra from subaerial and submarine silicic eruptions in the Kermadec arc: implications for eruption processes and dredge sampling. Bulletin of Volcanology 74(6): 1425-1443.

Benage MC, Dufek J, Degruyter W, Geist D, Harpp K, Rader E 2014. Tying textures of bread crust bombs to their transport regime and cooling history. Journal of Volcanology and Geothermal Research 274: 92-107.

Bottinga Y, Weill DF 1972. The viscosity of magmatic silicate liquids; a model calculation. American Journal of Science 272(5): 438-475.

Branney MJ, Kokelaar BP 2002. Pyroclastic density currents and the sedimentation of ignimbrites. London, Geological Society.

Brown RJ, Andrews GD 2015. Deposits of Pyroclastic Density Currents In: Sigurdsson H, Houghton BF, McNutt S, Rymer H, Stix J ed. Encyclopedia of Volcanoes. Second ed. San Diego, Academic Press. Pp. 631-648.

Buchwaldt R 2013. Pyroclastic Flow. Encyclopedia of Natural Hazards.

Buckland HM, Eychenne J, Rust AC, Cashman KV 2018. Relating the physical properties of volcanic rocks to the characteristics of ash generated by experimental abrasion. Journal of Volcanology and Geothermal Research 349: 335-350.

Carracedo Sánchez M, Sarrionandia F, Arostegui J, Eguiluz L, Gil Ibarguchi JI 2012. The transition of spatter to lava-like body in lava fountain deposits: features and examples from the Cabezo Segura volcano (Calatrava, Spain). Journal of Volcanology and Geothermal Research 227-228: 1-14.

Cole JW 1990. Structural control and origin of volcanism in the Taupo volcanic zone, New Zealand. Bulletin of Volcanology 52(6): 445-459.

Conway CE, Leonard GS, Townsend DB, Calvert AT, Wilson CJN, Gamble JA, Eaves SR 2016. A high-resolution 40Ar/39Ar lava chronology and edifice construction history for Ruapehu volcano, New Zealand. Journal of Volcanology and Geothermal Research 327: 152-179.

Cowlyn JD 2016. Pyroclastic density currents at Ruapehu volcano; New Zealand. PhD Thesis, University of Canterbury 268 p.

Cronin SJ, Lube G, Dayudi DS, Sumarti S, Subrandiyo S, Surono 2013. Insights into the October-November 2010 Gunung Merapi eruption (Central Java, Indonesia) from the stratigraphy, volume and characteristics of its pyroclastic deposits. Journal of Volcanology and Geothermal Research 261: 244-259.

Donoghue SL, Gamble JA, Palmer AS, Stewart RB 1995. Magma mingling in an andesite pyroclastic flow of the Pourahu Member, Ruapehu volcano, New Zealand. Journal of Volcanology and Geothermal Research 68(1): 177-191.

Eaves SR 2015. The glacial history of Tongariro and Ruapehu volcanoes, New Zealand. PhD Thesis, Victoria University of Wellington. 286 p.

Eaves SR, Mackintosh AN, Anderson BM, Doughty AM, Townsend DB, Conway CE, Winckler G, Schaefer JM, Leonard GS, Calvert AT 2016. The Last Glacial Maximum in the central North Island, New Zealand: Palaeoclimate inferences from glacier modelling. Climate of the Past 12(4): 943-960.

Fisher RV, Schmincke H-U 1984. Pyroclastic rocks. Berlin, Springer.

Gamble JA, Wood CP, Price RC, Smith IEM, Stewart RB, Waight T 1999. A fifty year perspective of magmatic evolution on Ruapehu Volcano, New Zealand: verification of open system behaviour in an arc volcano. Earth and Planetary Science Letters 170(3): 301-314.

Hackett WR 1985. Geology and Petrology of Ruapehu Volcano and Related Vents. PhD Thesis, Victoria University of Wellington.

Hackett WR, Houghton BF 1989. A facies model for a quaternary andesitic composite volcano: Ruapehu, New Zealand. Bulletin of Volcanology 51(1): 51-68.

Hall ML, Steele AL, Bernard B, Mothes PA, Vallejo SX, Douillet GA, Ramón PA, Aguaiza SX, Ruiz MC 2015. Sequential plug formation, disintegration by Vulcanian explosions, and the generation of granular Pyroclastic Density Currents at Tungurahua volcano (2013–2014), Ecuador. Journal of Volcanology and Geothermal Research 306: 90-103.

Hiroi Y, Miyamoto T 2016. Relationship between eruptive style and vesicularity of juvenile clasts during eruptive episode A of Towada Volcano, Northeast Japan. Journal of Volcanology and Geothermal Research 325: 86-97.

Houghton BF, Wilson CJN 1989. A vesicularity index for pyroclastic deposits. Bulletin of Volcanology 51(6): 451-462.

Houghton BF, Gonnermann HM 2008. Basaltic explosive volcanism: Constraints from deposits and models. Chemie der Erde - Geochemistry 68(2): 117-140.

Jenkins S, Komorowski JC, Baxter PJ, Spence R, Picquout A, Lavigne F, Surono 2013. The Merapi 2010 eruption: An interdisciplinary impact assessment methodology for studying pyroclastic density current dynamics. Journal of Volcanology and Geothermal Research 261: 316-329.

Johnston DM, Neall VE 1995. Ruapehu Awakens: The 1945 Eruption of Ruapehu. The Science Centre and Manawatu Museum Scientific Monograph(1): 28.

Johnston DM, Houghton BF, Neall VE, Ronan KR, Paton D 2000. Impacts of the 1945 and 1995-1996 Ruapehu eruptions, New Zealand: An example of increasing societal vulnerability. Geological Society of America Bulletin 112(5): 720-726.

Jutzeler M, Proussevitch AA, Allen SR 2012. Grain-size distribution of volcaniclastic rocks 1: A new technique based on functional stereology. Journal of Volcanology and Geothermal Research 239-240: 1-11.

Kilgour G, Blundy J, Cashman K, Mader HM 2013. Small volume andesite magmas and melt–mush interactions at Ruapehu, New Zealand: evidence from melt inclusions. Contributions to Mineralogy and Petrology 166(2): 371-392.

Kilgour GN, Mader HM, Blundy JD, Brooker RA 2016. Rheological controls on the eruption potential and style of an andesite volcano: A case study from Mt. Ruapehu, New Zealand. Journal of Volcanology and Geothermal Research 327: 273-287.

Knight PG 1999. Glaciers. New York, Franklin Watts.

Kueppers U, Putz C, Spieler O, Dingwell DB 2012. Abrasion in pyroclastic density currents: Insights from tumbling experiments. Physics and Chemistry of the Earth 45-46: 33-39.

Lube G, Cronin SJ, Platz T, Freundt A, Procter JN, Henderson C, Sheridan MF 2007. Flow and deposition of pyroclastic granular flows: A type example from the 1975 Ngauruhoe eruption, New Zealand. Journal of Volcanology and Geothermal Research 161(3): 165-186.

Manville V, Hodgson KA, Houghton BF, Keys JR, White JDL 2000. Tephra, snow and water: complex sedimentary responses at an active snow-capped stratovolcano, Ruapehu, New Zealand. Bulletin of Volcanology 62(4): 278-293.

Mellors RA, Sparks RSJ 1991. Spatter-rich pyroclastic flow deposits on Santorini, Greece. Bulletin of Volcanology 53(5): 327-342.

Nairn IA, Self S 1978. Explosive eruptions and pyroclastic avalanches from Ngauruhoe in February 1975. Journal of Volcanology and Geothermal Research 3(1): 39-60.

Nairn IA, Scott BJ, Ruapehu Surveillance G 1996. Volcanic eruption at a New Zealand ski resort prompts reevaluation of hazards. Eos 77(20): 189-191.

Newhall C, Hoblitt R 2002. Constructing event trees for volcanic crises. Bulletin of Volcanology 64(1): 3-20.

Newhall CG, Self S 1982. The volcanic explosivity index (VEI) - an estimate of explosive magnitude for historical volcanism. Journal of Geophysical Research-Oceans 87(NC2): 1231-1238.

Pardo N 2012. Andesitic Plinian eruptions at Mt. Ruapehu (New Zealand): From lithofacies to eruption dynamics. PhD Thesis, Massey University.

Pardo N, Cronin SJ, Palmer AS, Németh K 2012a. Reconstructing the largest explosive eruptions of Mt. Ruapehu, New Zealand: lithostratigraphic tools to understand subplinian–plinian eruptions at andesitic volcanoes. Bulletin of Volcanology 74(3): 617-640.

Pardo N, Cronin S, Palmer A, Procter J, Smith I 2012b. Andesitic Plinian eruptions at Mt. Ruapehu: quantifying the uppermost limits of eruptive parameters. Bulletin of Volcanology 74(5): 1161-1185.

Pardo N, Cronin SJ, Wright HMN, Schipper CI, Smith I, Stewart B 2014. Pyroclast textural variation as an indicator of eruption column steadiness in andesitic Plinian eruptions at Mt. Ruapehu. Bulletin of Volcanology 76(5): 1-19.

Price RC, Gamble JA, Smith IEM, Maas R, Waight T, Stewart RB, Woodhead J 2012. The anatomy of an andesite volcano: A time-stratigraphic study of andesite petrogenesis and crustal evolution at Ruapehu Volcano, New Zealand. Journal of Petrology 53(10): 2139-2189.

Roche O, Phillips JC, Kelfoun K 2013. Pyroclastic density currents. In: Fagents SA, Gregg TKP, Lopes RMC ed. Modeling volcanic processes: the physics and mathematics of volcanism. Cambridge, Cambridge University Press.

Rodríguez-Elizarrarás S, Siebe C, Komorowski J-C, Espíndola JM, Saucedo R 1991. Field observations of pristine block- and ash-flow deposits emplaced April 16–17, 1991 at Volcán de Colima, Mexico. Journal of Volcanology and Geothermal Research 48(3): 399-412.

Rosi M, Paladio-Melosantos M, Di Muro A, Leoni R, Bacolcol T 2001. Fall vs flow activity during the 1991 climactic eruption of Pinatubo Volcano (Philippines). Bulletin of Volcanology 62(8): 549-566.

Scott BJ 2013. A revised catalogue of Ruapehu volcano eruptive activity: 1830-2012. Taupo, New Zealand, GNS Science.

Stinton AJ, Sheridan MF 2008. Implications of long-term changes in valley geomorphology on the behavior of small-volume pyroclastic flows. Journal of Volcanology and Geothermal Research 176(1): 134-140.

Thouret JC, Ramirez JC, Gibert-Malengreau B, Vargas CA, Naranjo JL, Vandemeulebrouck J, Valla F, Funk M 2007. Volcanoglacier interactions on composite cones and lahar generation: Nevado del Ruiz, Colombia, case study. Annals of Glaciology 45(1): 115-127.

Tost M, Cronin SJ 2015. Linking distal volcaniclastic sedimentation and stratigraphy with the development of Ruapehu volcano, New Zealand. Bulletin of Volcanology 77(11): 1-17.

Townsend DB, Leonard GS, Conway CE, Eaves SR, Wilson CJN 2017. Geology of the Tongariro National Park Area. GNS Science Geological Map 4. 1 sheet + 109 p.

Valentine GA, Perry FV, WoldeGabriel G 2000. Field characteristics of deposits from spatter-rich pyroclastic density currents at Summer Coon volcano, Colorado. Journal of Volcanology and Geothermal Research 104(1-4): 187-199.

Walker GPL 1971. Grain-Size Characteristics of Pyroclastic Deposits. The Journal of Geology 79(6): 696-714.

Walker GPL, Croasdale R 1971. Characteristics of some basaltic pyroclastics. Bulletin Volcanologique 35(2): 303-317.

Wilson CJN 1991. Ignimbrite morphology and the effects of erosion: a New Zealand case study. Bulletin of Volcanology 53(8): 635-644.

Wilson CJN, Houghton BF, McWilliams MO, Lanphere MA, Weaver SD, Briggs RM 1995. Volcanic and structural evolution of Taupo Volcanic Zone, New Zealand: a review. Journal of Volcanology and Geothermal Research 68(1): 1-28.

Witham CS 2005. Volcanic disasters and incidents: A new database. Journal of Volcanology and Geothermal Research 148(3): 191-233.